2002

Integrating response surface methods and uncertainty analysis into ship concept exploration

Price, Shelly L. (Shelly Loustaunau)

Monterey California. Naval Postgraduate School

Integrating Response Surface Methods and Uncertainty Analysis into Ship Concept Exploration

by

Shelly L. Price

B.S. Mechanical Engineering
United States Naval Academy, 1996

Submitted to the Department of Ocean Engineering and the Department of Mechanical Engineering in Partial Fulfillment of the Requirements for the Degrees of

Naval Engineer

and

Master of Science in Mechanical Engineering

at the
Massachusetts Institute of Technology

June 2002

Signature of Author Shelly L Price
Department of Ocean Engineering and the
Department of Mechanical Engineering
May 15, 2002

Certified by
Clifford A. Whitcomb, Senior Lecturer
Engineering Systems Division
Thesis Supervisor

Certified by
Martin L. Culpepper
Assistant Professor of Mechanical Engineering
Thesis Reader

Accepted by
Henrik Schmidt, Professor of Ocean Engineering
Chairman, Department Committee on Graduate Students
Department of Ocean Engineering

Accepted by
Ain A. Sonin, Professor of Mechanical Engineering
Chairman, Department Committee on Graduate Students
Department of Mechanical Engineering

Page Intentionally Left Blank

Integrating Response Surface Methods and Uncertainty Analysis into Ship Concept Exploration

by

Shelly L. Price

Submitted to the Department of Ocean Engineering and the Department of Mechanical Engineering in Partial Fulfillment of the Requirements for the Degrees of
Naval Engineer
and
Master of Science in Mechanical Engineering

ABSTRACT

The concept design phase of any type of ship determines the hull form, baseline capabilities, and a large portion of the total program cost. The complexity of the ship design process leads to numerous assumptions and a great deal of uncertainty in the point designs during the concept exploration phase. While it is not feasible to eliminate this uncertainty, it is useful to explore how it affects the overall design. An analysis of the uncertainty associated with each point design provides the designer with additional information for comparing designs.

It is important to consider all options and choose the baseline design that best meets the customer's requirements. Current trade-off studies tend to examine a few point designs that may or may not cover the entire design space. This approach relies heavily on designer experience, is inefficient, and may not lead to an optimum baseline design. Response Surface Methods (RSM) provide statistical tools for determining the relationships between factors (inputs) and responses (outputs). When combined with Design of Experiments (DOE), this approach allows the designer to thoroughly investigate the design space using relatively few point designs. The benefit of this analysis is the ability to efficiently examine the effects of changing factors on the overall design.

Finally, the combination of RSM and an uncertainty analysis gives the designer a tremendous understanding of the design space. The thesis develops a method allowing the designer to make important decisions, such as hull form or basic mission capabilities of the ship, explicitly showing the uncertainty associated with key design parameters.

Thesis Supervisor: Clifford A. Whitcomb,
Title: Senior Lecturer, Engineering Systems Division

Thesis Reader: Martin L. Culpepper,
Title: Assistant Professor of Mechanical Engineering

Page intentionally left blank

TABLE OF CONTENTS

LIST OF FIGURES

LIST OF TABLES

Page intentionally left blank

CHAPTER 1: INTRODUCTION

The ship design process has been described as a "multi-dimensional web of interacting closed loops" [1], pointing out the high level of complexity involved. While it is a difficult task to design any ship given the highly coupled nature of the complex interactions, it becomes even more difficult to create a design that can effectively meet multiple sets of potentially conflicting requirements. The design space, and any associated objective function, is non-linear, discontinuous and bounded by a variety of constraints preventing the application of gradient-based optimization techniques such as Lagrange multipliers, steepest ascent methods, linear programming, non-linear programming and dynamic programming. In addition, uncertainty in determination of design variables in the early stages of design adds yet another layer of difficulty in searching for solutions. This thesis develops and presents a method to allow exploration of a complex, highly coupled design space that explicitly takes uncertainty in design variables into consideration in determining the best system-level solution without the need for explicit determination of an objective function.

1.1 CONCEPT EXPLORATION

During the Cold War, the ship concept exploration process was somewhat simplified in that productivity and risk avoidance were the key factors in the process. New ideas took a backseat to the need for fast-paced ship production and were not thoroughly investigated. Since the end of the Cold War, however, tighter budgets and acquisition reform have made Navy leaders more interested in new technologies and ideas that may improve the operational effectiveness and cost efficiency of the ships [2].

The ultimate goal of concept exploration is to develop a baseline design that will meet the requirements laid out by the customer. Many key decisions are made, which have a tremendous impact on the completed ship. In fact, it is estimated that over 80% of the ship's acquisition cost is determined by decisions made during the concept exploration phase [3]. It is easy to see why this is true. This baseline is the starting point for the rest of the design process, making it imperative that it is an efficient platform to meet the customer requirements.

With so many key decisions to be made during concept exploration, the decision-makers obviously want as much detailed information about each idea as possible. This poses a problem for the designer, because with hundreds of possible concepts to explore, there is never enough time or resources to fully explore all of them. This means that the decisions must be made with only cursory studies into several of the concepts, making concept exploration that much more difficult.

1.2 Design Requirements

Obviously, the design requirements play a vital role in the ship concept selection. In a simple problem, the requirements would be very well defined, and the optimal design would be the one that best measures up to the design requirements. The ship design process, however, is far from being a simple problem. Even if the requirements are clearly defined, the existence of multiple conflicting criteria and non-availability of an objective function based on design variables compounds the complexity of the design space, preventing the use of optimization techniques such as Lagrange multipliers or steepest ascent methods, among others.

The need for interaction with the customer, who naturally wants a high performance ship, but may not understand the feasible limits of technology, further complicates the problem. Range, speed and payload requirements can be used as an example. In a multiple criteria sense, it is impossible to maximize all three of these attributes at the same time. A ship with a long range and large payload would be very large, making it difficult to achieve high speeds. The existence of multiple decision criteria leads to the question of what the customer's priorities are. If they are most concerned with speed, they must be willing to sacrifice either range or payload, or both, to the limitations of their budget or the limitations of the physics of the problem. It is very difficult for a customer to articulate these priorities, because they are highly dependent on the amount of any criterion that must be sacrificed. Questions such as "how much would payload be reduced in order to increase the speed by 3 kts" are common, and can be difficult for the designer to answer.

Due to the need for customer preference input, the designer cannot work alone during the concept exploration phase. In order to select the baseline design, the designer must identify several cost-effective solutions and present them to the decision-maker for the final decision [3].

1.3 Current Practice

In the earliest stages of the concept exploration phase, the designer must take the customer requirements, and estimate various parameters for the ship. The design process is often represented by a spiral, as shown in Figure 1. The first time around the spiral, each parameter is estimated. Subsequent trips around the spiral lead to refinement of these estimates, and the design eventually converges at the center [4].

Concept exploration can begin once a balanced design has been created. It is currently an *ad hoc* process, which is guided mainly by designer experience [3]. The designer compares the baseline to the requirements, and then adjusts one factor at a time in an attempt to improve the performance of the ship. These excursions can be scored and compared, but they may not cover the entire design space of interest. There is currently no efficient method for searching the design space for acceptable solutions.

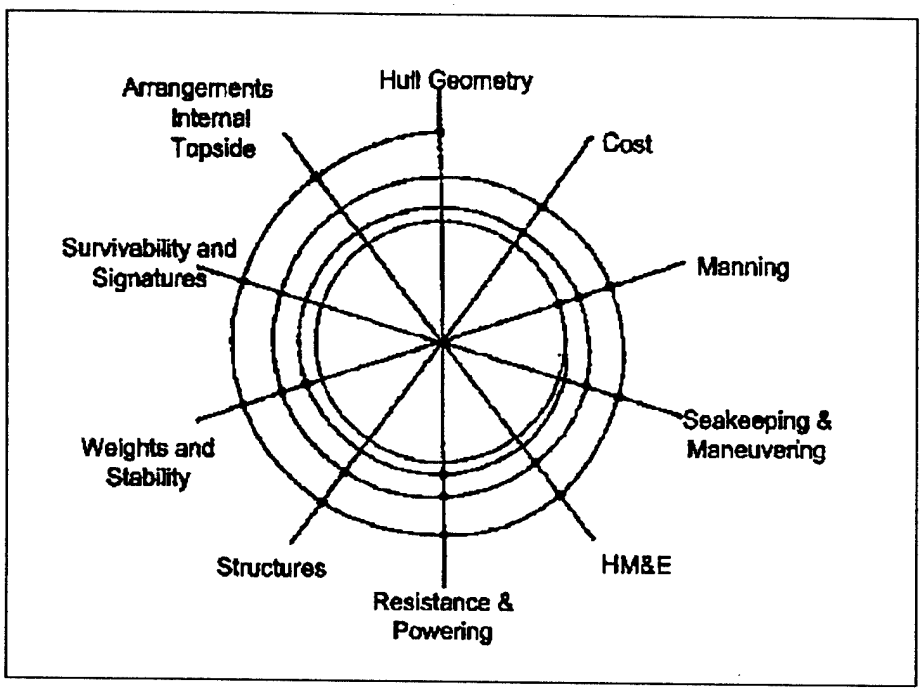

Figure 1: Design Spiral

1.3.1 Modeling Customer Preference

In order for the designer to select from among feasible solutions using the requirements as the basis for the decision, customer preference must be considered. Since customers are not available for direct interaction with the designer, a model must

be used. A single metric, the Overall Measure of Effectiveness (OMOE) of a ship is used in this thesis and comes directly from the customer requirements. The major performance areas identified in the requirements must be broken into quantifiable attributes. The attribute scores for each concept are combined to create the OMOE, which can be used to judge the design's goodness. There are several existing methods for calculating the OMOE of a ship, including a weighted sum, hierarchical weighted sum, analytic hierarchy process, and multiattribute utility analysis. Reference 5 provides a summary of each of these methods.

1.3.2 Pareto Boundary

Whenever designers deal with multiple, conflicting criteria, consideration of Pareto optimality is required. The Pareto optimal solution set is defined as the set of points where there is no way to improve one criterion without degrading another. This solution set is also referred to as the set of non-dominated solutions. A useful method for comparing the cost-effectiveness of different designs is plotting the OMOE vs. cost of each variant as a Pareto plot [5]. A sample plot is shown in Figure 2. The ideal point on this plot is in the upper left corner, where the maximum OMOE is achieved for the minimum cost. As point designs are added to this plot, the Pareto optimal boundary solution set becomes evident, and is represented by the dashed line in the figure. For each point design along this line, there is no solution that can improve both the cost and the OMOE of the ship simultaneously. Any reduction in cost must lead to a decrease in OMOE, and any increase in OMOE must lead to an increase in cost. The solutions falling below the Pareto boundary are called dominated solutions. For each of these designs, another design exists with both a higher OMOE and lower cost. It is important

to note that the Pareto boundary does not identify a single optimal solution, but rather identifies the set of non-dominated solutions. Choosing among these non- dominated solutions is a matter of customer preference [5].

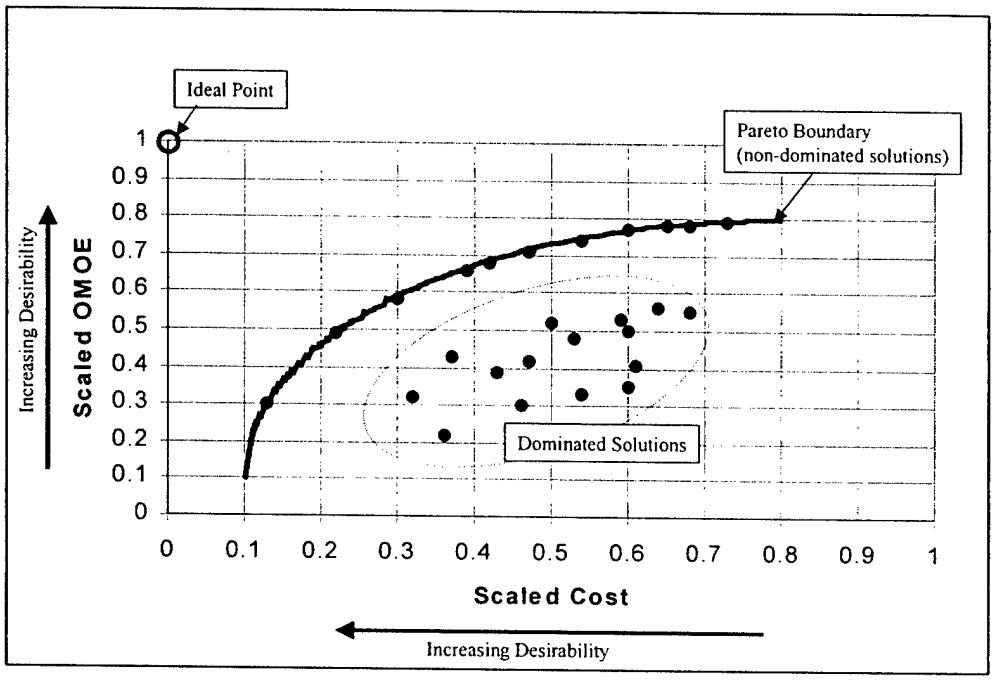

Figure 2: OMOE vs. Cost Plot

This type of plot is a very useful decision-making tool, but it has limitations. First, determining the Pareto boundary requires a large number of point designs, each of which takes time and money. With so many designs, there is no guarantee that the point designs represented in the plot cover the entire design space. This means that designs could exist that change the shape of the Pareto boundary. Also, the huge amount of uncertainty involved in a concept design actually creates ambiguity in the boundaries of each point. Many designs with a high OMOE and low cost depend on new technologies with much higher levels of uncertainty. Therefore, the cost and OMOE of the completed

ship may have changed so much that the design is actually a dominated solution. OMOE vs. cost plots are unable to display any uncertainties associated with the designs. Finally, each point on the plot is static, and there is no way to interpolate in between designs. It is impossible to answer questions about how changing certain factors will affect the design.

1.4 Areas for Improvement

The first step in ensuring that the concept exploration phase ends with a suitable baseline design that is robust to the customer requirements is ensuring that the entire design space is investigated. This means that different factors and their ranges of possible values must be identified early in the process, so the design space can be appropriately bounded. Additionally, in cases where the design space is nonlinear and/or discontinuous, as with different hull forms, multiple design spaces must be considered. This approach requires a considerable amount of initial planning, but the return is well worth the investment. Once the design space has been defined by a number of factors, one of many Design of Experiments (DOE) methods may be used to find the minimum number of variants to cover the space.

Analyzing the effects of uncertainty involved in the synthesis model, as well as in the cost and OMOE models, on the overall design can provide the decision-maker with important information about each variant. Instead of each parameter in the design being represented by a single value, each can be represented by a probability distribution, allowing the level of uncertainty to be tracked throughout the synthesis process. Displaying the uncertainty levels associated with each variant on an OMOE vs. cost plot allow the decision-maker to see which variants have the most inherent uncertainty.

Finally, it would be very helpful for the designer to have the ability to answer various "what if" questions about design parameters. For example, the decision-maker may like a certain design, but want to know how fast it would be able to go if an additional 50 ltons of payload was added. Currently, the designer would have to adjust some factors and proceed through the entire design spiral to answer that question. Response Surface Methods (RSM) is a statistical tool that enables the designer to interpolate between point designs, thus allowing rapid answers to a variety of "what-if" questions.

Combining the OMOE tools currently in use with uncertainty analysis, DOE and RSM creates a powerful decision-making environment in which the entire design space can be fully explored. This approach does not attempt to identify a single, optimal solution, but rather presents several non-dominated solutions in a format where they can be easily compared. The result is more informed decisions during concept exploration, which ultimately produce a more effective and efficient ship design.

CHAPTER 2: SOURCES OF UNCERTAINTY

In order to generate the point designs to accomplish investigation of the entire design space during concept exploration, the designer must rely on a synthesis tool. Additionally, each design must be evaluated using an OMOE, and a cost. All of these models introduce some uncertainty into the process, as discussed in the following sections.

2.1 SYNTHESIS MODEL

It is not difficult to see where the uncertainty in the synthesis model comes from. Most models rely on assumptions to determine weights, resistance characteristics, and even the hull form itself. These assumptions are usually drawn from past experience in ship design, and can be very accurate for current technologies. The big problem arises when a new technology, which may not be fully developed during the concept design phase, is to be incorporated into the ship. In this case, the designer must make an educated guess as to the weight, space or resistance impacts the new system will have on the design, or must undertake expensive scale model tests to collect data to update the synthesis models. To ensure that the design is flexible enough to survive the entire process, large margins and safety factors are routinely used.

2.1.1 EXAMPLE: CONVENTIONAL MONOHULL RESISTANCE

Calculating the resistance and required power for a monohull provides a good example of how uncertainty enters into the synthesis tool. The resistance characteristics of a monohull are well established, with plenty of information to support the assumptions in the model. This is not the case with several advanced hull forms, which are only

beginning to be built and tested, and for which the design information is mostly proprietary.

This example shows a basic resistance and powering calculation for a frigate and points out several sources of uncertainty. The resistance and required power calculations are based on those of the MIT Math Model, but all calculations are done with a Microsoft® Excel spreadsheet using Crystal Ball® to run a Monte Carlo simulation. The sections below describe the sources of uncertainty associated with frictional, wave making, appendage and air resistance, and how they are defined in the model. Like many concept level models, this model ignores the effects of trim and shallow water on the resistance of the ship.

The MIT Math Model includes a 10 % power margin factor to the estimated effective horsepower (EHP), probably based on the U.S. Navy standard design procedures, to account for uncertainty in the model. An investigation of the uncertainty involved in the resistance model gives the designer a better understanding of the EHP probability distribution and may eliminate the need for a standard power margin factor. In this example, the 10% power margin factor is not included.

Ship Characteristics:

Since a model with this resolution would be used very early in the concept phase of the design, there is a great deal of uncertainty in the basic ship characteristics. Table 1 lists the characteristics of the frigate used in the example.

Table 1: Characteristics of Frigate

Parameter	Value	Distribution
Length (L)	408 ft	None
Beam (B)	45 ft	None
Depth at Station 10 (D_{10})	30 ft	None
Prismatic Coefficient (C_P)	.596	None
Max Section Coefficient (C_X)	.749	None
Full Load Displacement (Δ_{FL})	3500 – 4000 lton	Uniform

The draft is calculated using the following equation:

$$T = \frac{35 \cdot \Delta_{FL}}{C_P \cdot C_X \cdot L \cdot B} \tag{1}$$

Since draft depends on full load displacement, it also has a uniform distribution.

Frictional Resistance:

Frictional resistance ($R_{friction}$) for a ship can be calculated using a relatively simple formula:

$$R_{friction} = \frac{1}{2} \cdot \rho_{SW} \cdot S_S \cdot V_S^3 \cdot (C_A + C_F) \tag{2}$$

where: ρ_{SW} = density of seawater

S_S = ship wetted surface area

V_S = sustained speed of ship

C_A = correlation allowance (0.0004 for ships between 50 and 100 m in length)

C_F = frictional resistance coefficient

The density of seawater and the correlation allowance are assumed to be constant, as is the sustained speed of the ship, which is derived from the requirements. These three variables do not introduce any uncertainty into the calculation.

The wetted surface area of the ship introduces considerable uncertainty into the model. At this point in the design process, even if the basic dimensions of the ship are known, hull offsets may not exist, making it impossible to determine the exact wetted surface area. It can be estimated, however, using a coefficient read from the plot in Figure 3. In the figure, the surface coefficient (C_S) is dependent on the prismatic coefficient (C_P), which is constant, and the beam to draft ratio (B/T), which has some distribution. In this example, B/T is uniformly distributed between 2.6 and 3, so C_S is given a uniform distribution between 2.53 and 2.54.

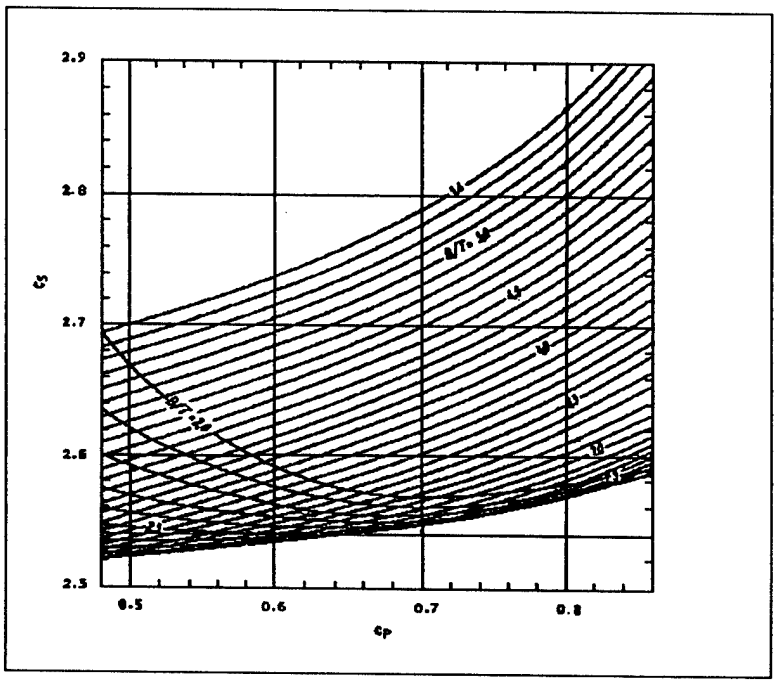

Figure 3:Wetted Surface Area Coefficient

The accepted method for calculating the frictional resistance coefficient (C_F) of a monohull is the ITTC equation (Eq.3), which is a curve fit based on data from various

ships. There are several alternate equations that yield similar, but not the same, results. A few of these are listed below:

ITTC Line: $$C_F = \frac{0.075}{(\log_{10} R_n - 2)^2} \quad (3)$$

ATTC Line: $$\frac{0.242}{\sqrt{C_F}} = \log_{10}(R_n \cdot C_F) \quad (4)$$

Hughes Line: $$C_F = \frac{0.066}{(\log_{10} R_n - 2.03)^2} \quad (5)$$

Granville Line: $$C_F = \frac{0.0776}{(\log_{10} R_n - 1.88)^2} + \frac{60}{R_n} \quad (6)$$

For most Reynolds number (R_n) values, each line yields a C_F within 10% of the ITTC line. In the model, C_F is characterized by a triangular distribution. The value calculated using the ITTC line is the most likely value, with the upper and lower limits of the distribution at +/- 10%.

Using the Monte Carlo simulation provided by Crystal Ball®, the calculation is run 10,000 times, resulting in the frictional resistance having the distribution shown in Figure 4.

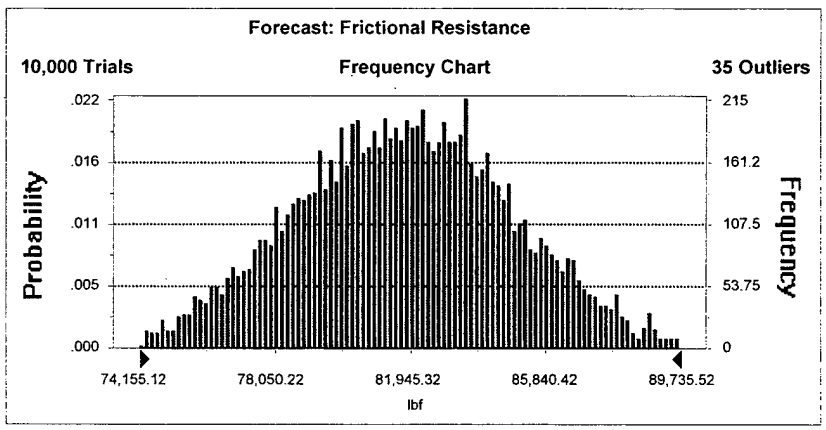

Figure 4: Frictional Resistance Probability Distribution

Residual Resistance:

The residual resistance is calculated using coefficients from reference 6, "A Reanalysis of the Original Test Data for the Taylor Standard Series" by Morton Gertler. This reference provides a series of curves for estimating the residual resistance coefficient (C_{RTSS}), given the speed-to-length ratio (R), C_V, C_P and B/T. Each curve is non-linear and depends on several variables. The estimates are derived from model tests of a parent hull and several offspring hulls. It is assumed that the same relationships apply to the hull in question, but if it deviates too much from the parent, this may not be a good assumption.

In the resistance model, C_P is constant, while C_V and B/T have distributions coming from the uncertainty in the ship's full load displacement and draft. The speed-to length ratio (R) is calculated for the sustained speed using the equation below.

$$R = \frac{V_S}{\sqrt{L}} \tag{7}$$

The residual resistance coefficients are recorded for each B/T (2.25, 3.0, 3.75), and assigned an appropriate distribution based on the range of C_V. Additional uncertainty comes from the fact that these values are read from a plot and are only as accurate as the human eye. Interpolation is required to determine the actual C_{RTSS}. In this model, C_{RTSS} at each B/T is assigned a uniform distribution. Using the Monte-Carlo simulation to repeat the calculation 10,000 times yields a probability distribution for the Taylor Standard Series residual resistance (R_{TSS}), which is calculated using the following equation:

$$R_{TSS} = \frac{1}{2} \cdot C_{RTSS} \cdot \rho_{SW} \cdot S_S \cdot V_S^2 \tag{8}$$

The Taylor Standard Series residual resistance must be corrected to account for differences between the hull in question and the parent hull using the Worm Curve Factor (WCF). It depends on R, and is read from the plot in Figure 5 and therefore has a distribution associated with the inaccuracies of the human eye. For the frigate, WCF is given a uniform distribution between 0.85 and 0.9.

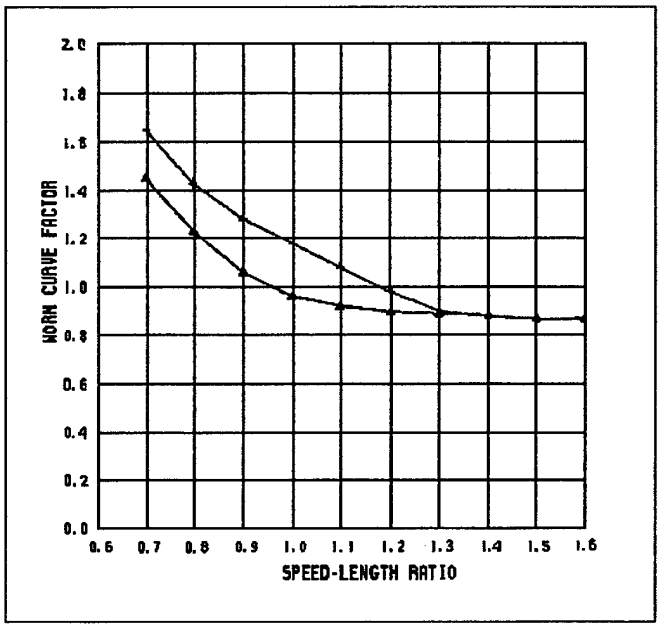

Figure 5: Recommended Worm Curves for USN Destroyer Type Hull Form without bow dome

The final residual resistance (R_R) is calculated as shown in equation 9 and is represented by the distribution shown in Figure 6.

$$R_R = R_{TSS} \cdot WCF \tag{9}$$

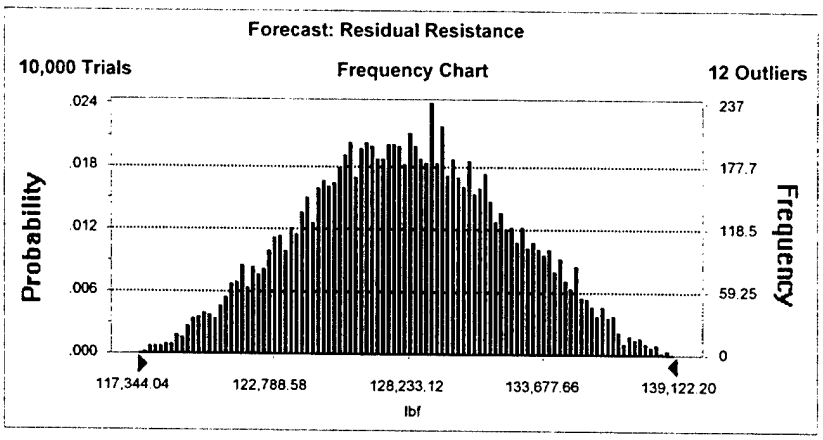

Figure 6: Residual Resistance Probability Distribution

Power Required to Overcome Bare Hull Resistance:

The bare hull resistance of the ship (R_{BH}) is simply the sum of the residual and frictional resistances. The power required to overcome the bare hull resistance is calculated as shown in equation 10. In this calculation, V_S is in ft/s, and the 550 is the conversion factor from lb-ft/s to hp.

$$P_{EBH} = \frac{R_{BH} \cdot V_S}{550} \tag{10}$$

The distribution of P_{EBH} is shown in Figure 7.

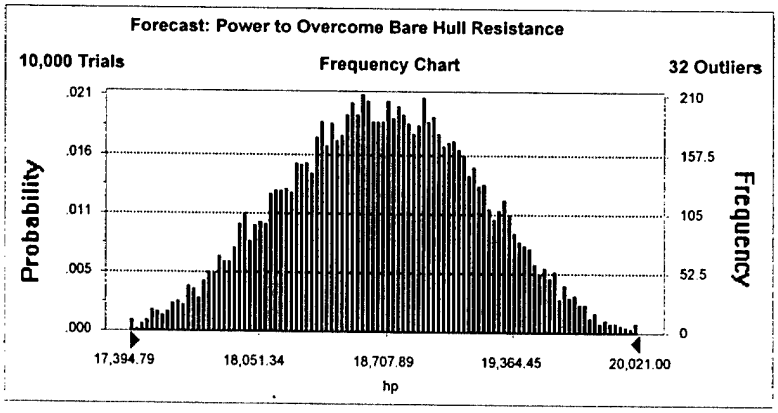

Figure 7: Power to Overcome Bare Hull Resistance Probability Distribution

Power Required to Overcome Appendage Drag:

The appendages of a ship include bilge keels, skegs, propellers, struts, shafts and possibly the sonar dome. In this model, only the sonar dome and propulsion system are considered. The sonar dome has a drag coefficient (C_{SD}) based on its shape. Since the coefficient must be estimated at this point in the design process, it is assigned a uniform distribution based on existing sonar dome data. In this case, it is between 0.110 and 0.119. The surface area of the sonar dome depends on the type of sonar, and is assumed to be constant. The power required to overcome the resistance of the sonar dome is calculated using equation 11. Again, V_S is in ft/s and 550 converts the result to hp.

$$P_{EAPPsd} = \frac{\frac{1}{2} \cdot C_{SD} \cdot \rho_{SW} \cdot A_{SD} \cdot V_S^3}{550} \tag{11}$$

The resistance associated with the propulsion system (propellers, struts, and shafts) is also significant, and must be considered. It can be estimated using an appendage drag coefficient (C_{DAPP}) read from Figure 8. It is important to note that this coefficient is not dimensionless, but has the units $\frac{hp \cdot 10^5}{ft^2 \cdot kt^2}$. Since C_{DAPP} is read from a plot, it is assigned a uniform distribution between 1.9 and 2.1.

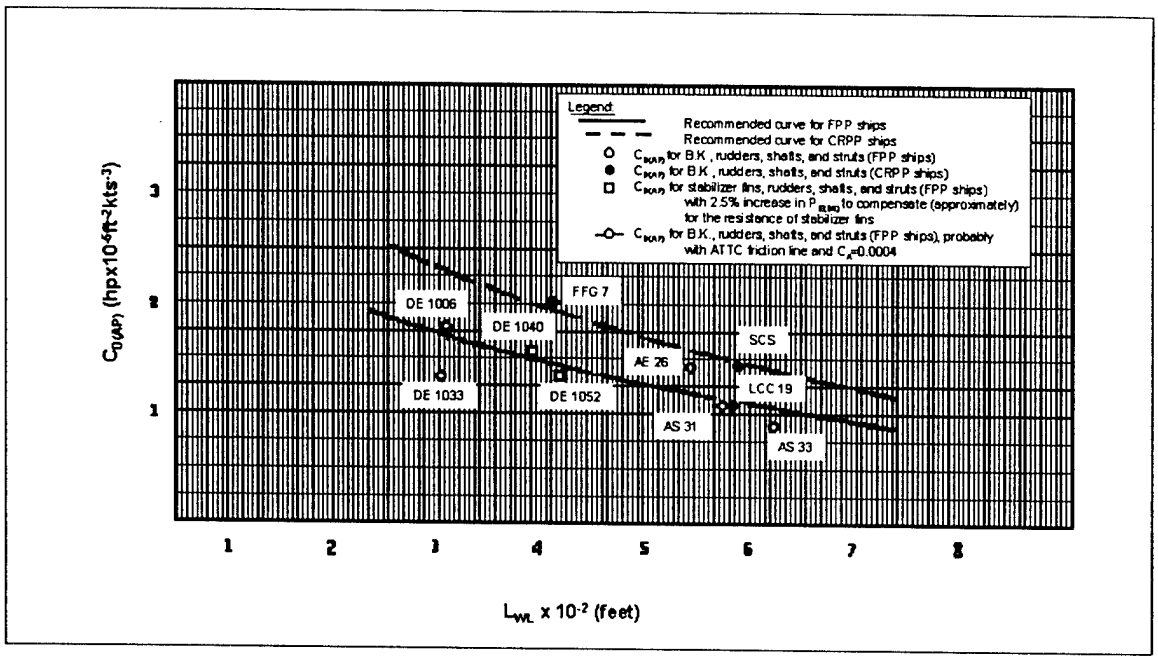

Figure 8: Appendage Drag Coefficient vs. Length

The power required to overcome the drag of the propeller, struts and shaft is calculated using equation 12. D_P is the propeller diameter (assumed to be constant), and the result is again converted to hp.

$$P_{EAPPp} = \frac{C_{DAPP} \cdot L \cdot D_P \cdot V_S^3}{550} \tag{12}$$

The total power required to overcome appendage drag is the sum of the power required to overcome the resistance of the sonar dome and the propulsion system. It has a distribution shown in Figure 9.

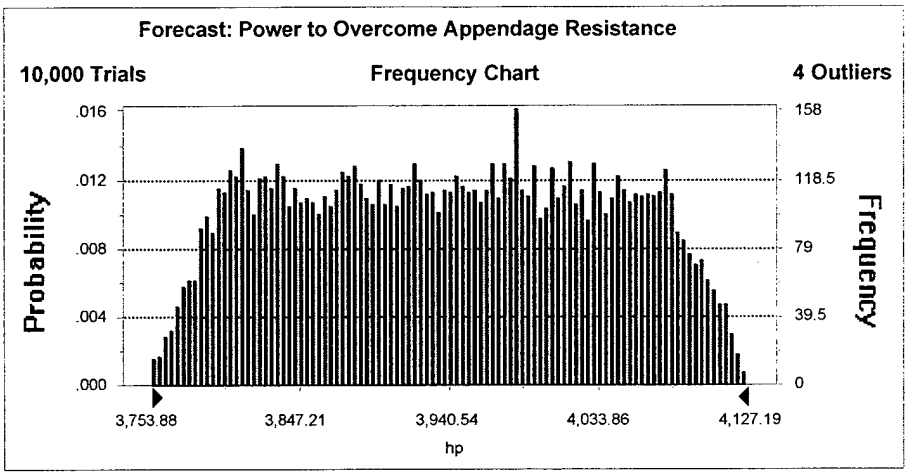

Figure 9: Power to Overcome Appendage Resistance Probability Distribution

Power Required to Overcome Air Resistance:

The power required to overcome air resistance (P_{EAA}) is calculated using equation 13.

$$P_{EAA} = \frac{1}{2} \cdot C_{AA} \cdot A_W \cdot \rho_A \cdot V_S^3 \tag{13}$$

where: C_{AA} = air drag coefficient

A_W = ship frontal area

ρ_A = density of air

The density of air is assumed to be constant in the model. The air drag coefficient depends on the shape of the ship's hull and deckhouse, making it difficult to know the exact value at this point in the design process. In this model, C_{AA} is assigned a uniform distribution between 0.065 and 0.075.

The ship's frontal area depends on the size and shape of the deckhouse, as well as the amount of freeboard the ship has. In the model, the deckhouse dimensions are

assumed to be constant, but the amount of freeboard depends on the draft of the ship, which has an associated distribution as discussed above.

Again using a Monte Carlo simulation, the power required to overcome air resistance is calculated, resulting in the distribution shown in Figure 10.

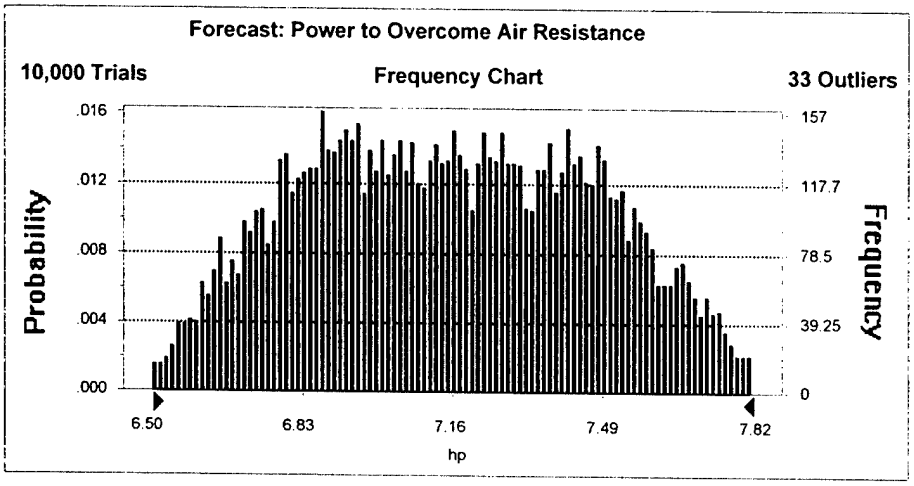

Figure 10: Power to Overcome Air Resistance Probability Distribution

Installed Horsepower Required:

The total effective horsepower required (EHP) is calculated in equation 14. In most current models, a power margin factor of approximately 10% of the EHP is added to the sum of the required powers calculated above. The purpose of the margin is to keep the design flexible enough to deal with the uncertainty in the model. Since this model tracks the uncertainty in the model, it is unnecessary to add the margin at this point.

$$EHP = P_{EBH} + P_{EAPPsd} + P_{EAPPp} + P_{EAA} \tag{14}$$

The EHP is divided by the propulsive coefficient (PC) to determine the required shaft horsepower (SHP), as shown in equation 15. The PC also has a probability

distribution associated with it, mainly due to the uncertainty in the propeller design. For this model, it is assumed to be a uniform distribution between 0.63 and 0.71.

$$SHP = \frac{EHP}{PC} \tag{15}$$

Finally, the required installed power (P_{IREQ}) is determined by adding an additional 25% to the SHP to allow for effects such as fouling and sea state. The probability distribution for P_{IREQ} is shown in Figure 11.

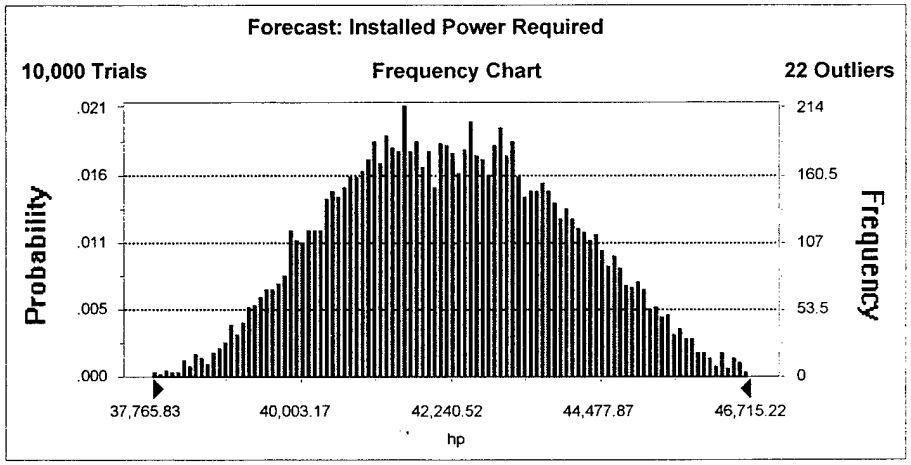

Figure 11: Installed Power Required Probability Distribution

A model that uses the 10% power margin factor instead of tracking the uncertainty throughout the model would calculate a required installed horsepower of 46,450 hp (the mean value is used for any factors with distributions described above). Comparing this value with the cumulative distribution of installed power shows that in this case, a design with 46,450 hp installed is a very conservative estimate, with greater than a 99% chance of meeting the sustained speed requirement of 29 kts. It is interesting to note that the actual installed power of a frigate is only 43,000 hp, a value that would

only have a 65% chance of meeting the speed requirement during the concept phase, pointing out the need to understand the uncertainty in the model.

A more detailed study in the different aspects of resistance would allow the designer to refine the distributions used for each factor.

2.1.2 Other Sources of Uncertainty in Synthesis Model

Other areas of the synthesis model also introduce large amounts of uncertainty into the design. Weight estimations are difficult during concept design due to a lack of information regarding the equipment that will be installed as well as the uncertainty in the structural design of the ship. Combat systems that will be installed in a ship are frequently at the concept design level themselves during the concept exploration of the ship, making it difficult to estimate their weights.

Similarly, it is very difficult to allocate the area and volume within the ship due to uncertainty in the equipment (both combat systems and propulsion). The crew size also plays an important role in the area and volume calculations. The crew size depends on both maintenance requirements of the equipment as well as operational requirements for watch-standing. The size of the crew determines the amount of berthing space required, as well as the fresh water and provisions requirements.

Uncertainty stems from other areas, as well, including electrical power requirements, stability and seakeeping. Obviously, every aspect of the ship is dependent on all the other aspects, making it extremely important to understand the propagation of uncertainty throughout the ship design.

2.2 Cost Model

The cost of a design at the concept level is always expected to have a great deal of uncertainty. Much of the uncertainty comes from the synthesis model and is simply propagated through the cost model. Other sources of uncertainty in the cost model include the Cost Estimating Ratios that are commonly used, as well as the unpredictable labor rates for construction. Even more uncertainty comes into play when new technology is added to the equation. A new hull type, for example, will undoubtedly cause several unforeseen problems that will delay the construction and cost money to solve.

For the purposes of this study, it is assumed that the cost model introduces no new uncertainty. Only the uncertainty from the synthesis model is considered.

2.3 OMOE Model

The model used to determine the OMOE of a ship design is typically very inexact for several reasons. Probably the most significant is that the future cannot be accurately predicted. Ships in the concept phase today will not be launched for 10 to 15 years, at which time the geopolitical environment of the world could be very different. It is therefore very difficult to determine what the requirements of future ships should be.

Even if a ship is designed to operate in a very well defined environment, there are differing opinions on what contributes to its effectiveness. This really shows up in a weighted sum OMOE model, in which various attributes are ranked and assigned a relative weighting. Customer surveys are often used to determine the relative weightings, but there is never complete agreement on the relative importance of the various attributes. The non-existence of a group utility function makes preference modeling more difficult.

Finally, there is again the uncertainty introduced by the synthesis model that is carried through the OMOE model. Again, this study focuses only on this type of uncertainty, and not uncertainty in the customer preference modeling.

CHAPTER 3: RESPONSE SURFACE METHODS

Several areas where the current concept exploration methods could be improved have been discussed. These include ensuring the entire design space is covered, and giving the designer the ability to quickly answer various "what-if" questions. Response Surface Methods (RSM) and Design of Experiments (DOE) can improve the process in both of these areas.

This chapter only outlines the basics of these methods. References 7 and 8 provide a more detailed explanation of the applications and the statistics involved.

3.1 OVERVIEW OF RSM/DOE

Response Surface Methods (RSM) are a statistical way of studying the empirical relationship between the factors (input variables that the designer would like to control) and measured responses (output variables that the decision maker would like to use in the selection process). The first step in applying Response Surface Methods to a problem is identifying the design space. The desired responses are determined, and then the factors must be carefully chosen. It is important that impact of the chosen factors on the responses is not overshadowed by other variables in the experiment. A poor choice of factors leads to large errors in the response surface, negating its usefulness. Screening experiments can be helpful at this stage to ensure significant factors are selected [9]. Additionally, the designer must determine the upper and lower limits of each factor. These limits directly affect the size of the design space. A very narrow range constrains the design space to a small region, but the large design space created by a very wide

range can cause large errors in the regression equations. In some cases, multiple design spaces must be utilized in order to study all possibilities.

3.1.1 Design of Experiments (DOE)

Once the design space has been clearly defined, combinations of factors must be selected and the experiment must be performed. DOE is used to select the minimum number of experiments that will lead to an accurate response surface over the design space. There are several existing templates for choosing point designs, including the Box-Behnken and Central Composite Designs. Both of these methods are tailored towards creating quadratic response surfaces, so they require three levels for each factor. Figure 12 shows the location of points in each design space for a three-factor design. The Central Composite Design method is the most common response surface design, and is accurate throughout the entire range of all factors due to the extreme points at the vertices. It is also useful when screening designs are a part of the experiment, since the screening designs can be used in the full analysis. Since the Box-Behnken does not have these extreme points, the surfaces will probably be less accurate in the corner regions. It is a very useful method, however, when the extreme points are not feasible [10].

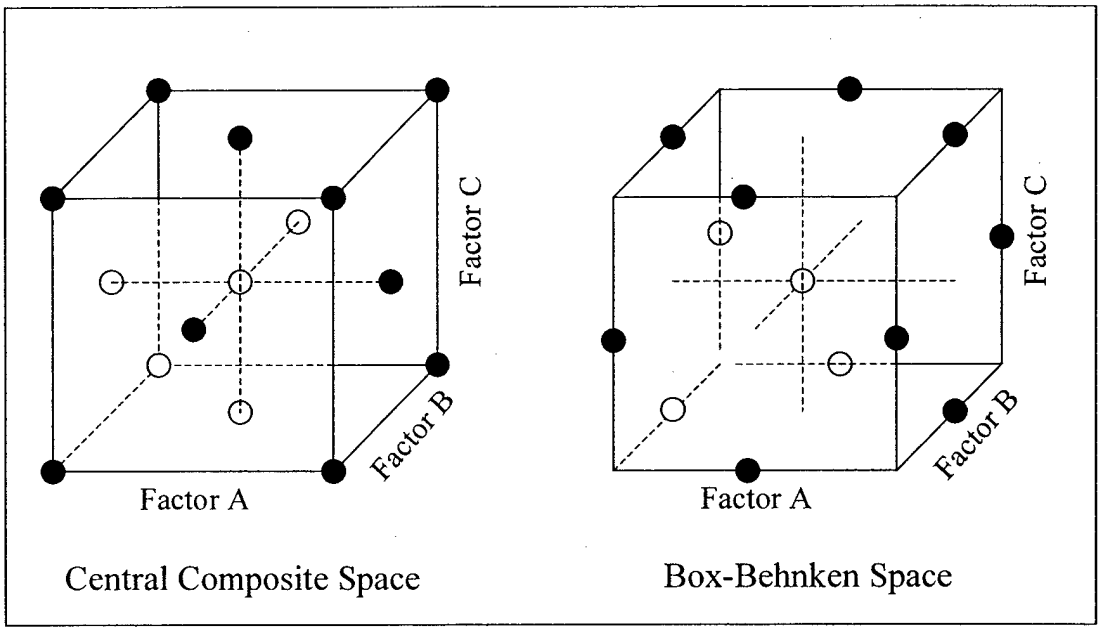

Figure 12: Box-Behnken and Central Composite Design Spaces

3.1.2 Response Surface Equations

An experiment is conducted for each combination of factors required by the chosen DOE. Using the measured responses from each experiment, it is possible to fit a multi-dimensional surface over the design space. A quadratic surface described by equation 16 is created for each response (y) [11].

$$y = b_0 + \sum_{i=1}^{k} b_i x_i + \sum_{i=1}^{k} b_{ii} x_i^2 + \sum_{i=1}^{k} \sum_{j=i+1} b_{ij} x_i x_j + \varepsilon \qquad (16)$$

where: b_0, b_i, b_{ii}, b_{ij} are coefficients obtained from multivariate regression

k is the number of factors (x)

ε is the error representing a lack of fit

It is important to pay attention to the error involved in each response surface. A large error indicates that the surface is not a very good representation of the set of data points,

meaning that the response surface will not be an accurate prediction tool. Reconsidering the factors chosen for the experiment to make sure they are the most significant contributors to the response can reduce the error. Additionally, changing the limits of the factors to reduce the size of the design space can often reduce the error.

Now, it is possible to use the response surface equation to estimate the response for combinations of factor values other than those included in an experiment. The simple example below illustrates the use of response surface methods in the ship design process.

3.2 RSM Example: Littoral Catamaran

RSM can be very useful in the concept exploration phase of the ship design process. In this example, RSM/DOE will be used to provide the decision-maker with information concerning the full load displacement and required installed horsepower for a littoral catamaran.

Translating the requirements for a ship into useable factors and responses can be a very difficult process requiring iterative interaction with the decision-maker, which is not addressed in this study. The factors and their upper and lower limits are listed in Table 2.

Table 2: Factor Limits for Littoral Catamaran Example

Factor	Lower Limit	Upper Limit
Speed	35 kts	50 kts
Payload	100 ltons	200 ltons
Range	1000 nm	2000 nm

The central composite method is the chosen DOE method due to its ability to accurately represent the entire design space. The required variants are listed in Table 3. The pattern column indicates which value is used for each factor, with "+" or "A" representing the upper limit, "-" or "a" representing the lower limit, and "0" representing

the midpoint. Each variant was balanced using a simple synthesis model, and the responses, full load displacement and required installed power were recorded.

Table 3: Catamaran Point Designs

Variant	Pattern	Speed	Payload	Range	SHP	Disp	Cost	OMOE
1	---	35	100	1000	10238.60	419.84	30.10	0.009
2	--+	35	100	2000	13152.10	539.31	36.38	0.339
3	a00	35	150	1500	17230.90	706.56	45.09	0.337
4	-+-	35	200	1000	20394.00	836.27	51.81	0.336
5	-++	35	200	2000	26220.90	1075.20	64.09	0.668
6	0a0	42.5	100	1500	15212.80	471.04	33.88	0.337
7	00a	42.5	150	1000	20283.70	628.05	42.38	0.338
8	0	42.5	150	1500	22819.20	706.56	46.60	0.504
9	00A	42.5	150	2000	26016.10	805.55	51.89	0.667
10	0A0	42.5	200	1500	30425.60	942.08	59.16	0.671
11	+--	50	100	1000	17464.30	419.84	32.19	0.342
12	+-+	50	100	2000	22433.90	539.31	38.94	0.670
13	A00	50	150	1500	29391.20	706.56	48.28	0.671
14	++-	50	200	1000	34786.70	836.27	55.46	0.670
15	+++	50	200	2000	44725.80	1075.20	68.56	1.000

3.2.1 Response Surfaces

The next step in the RSM process is using the data to generate the response surfaces. This step is done using a software package called JMP®. In addition to providing the equations for each response surface, it also provides statistical information about the curve fit. Equation 17 shows the response surface equation for the installed horsepower of the catamaran. In the equation, s represents the speed, p represents the payload, and r represents the range. It is important to note that the values for speed, payload and range are scaled so that the upper limit equals one and the lower limit equals negative one.

$$P_I = 22806.65 + 6156.54 \cdot s + 7805.13 \cdot p + 2938.15 \cdot r$$
$$+2048.763 \cdot s \cdot p + 771.038 \cdot s \cdot r + 985.363 \cdot p \cdot r \quad (17)$$
$$+507.533 \cdot s^2 + 15.683 \cdot p^2 + 346.38 \cdot r^2$$

The Actual by Predicted Plot and Summary of Variance provide a good summary of the accuracy of the curve fit. The Actual by Predicted Plot in Figure 13 shows how the values predicted by the model compare to the actual installed horsepower values. In a perfect fit, each point would fall exactly on a line with a slope of one. The plot shows that the installed horsepower response surface equation is very accurate, with an R-squared value of 1.00. The dashed lines on the plot represent the 95% confidence interval, which in this case is very close to the line representing a perfect model [11].

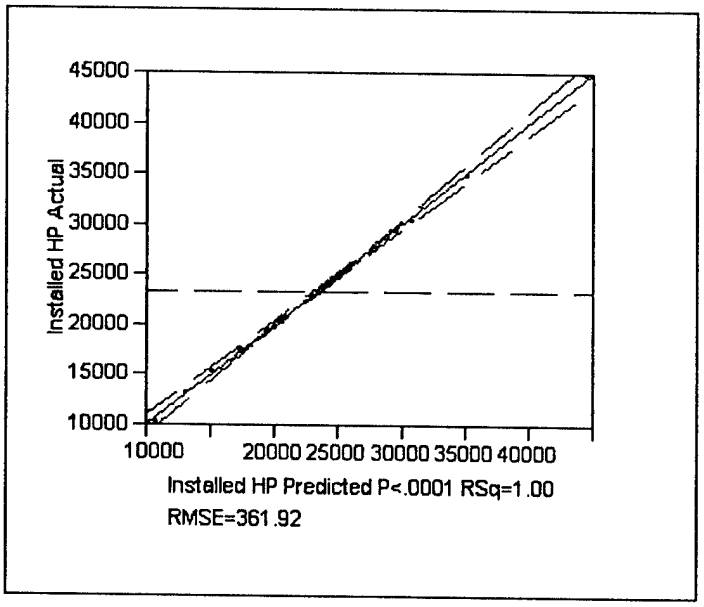

Figure 13: Installed Power Actual by Predicted Plot

The analysis of variance shown in Table 4 also gives important information regarding the fit of the response surface. The sum of squares and mean square of the model quantify the expected error from the curve fit of data. The unexplained error is

quantified in the error sum of squares and mean square. The F Ratio represents the ratio of the mean square of the model and the mean square of the error. "Prob > F" represents the probability that the F Ratio would be greater due to parameters in the synthesis model other than the factors. A very low "Prob > F" (on the order of 0.001) indicates that the main source of error is from the curve fit of the factors. A high "Prob > F" (on the order of 0.05 or greater), on the other hand, indicates that there is a great deal of error coming from other sources. This means that the difference in installed power for two ships designed using the same factor combination, such as 35 kts, 150 ltons, and 2000 nm, would be greater than the difference between this design and a ship designed to go 50 kts. In cases like this, the designer must try to improve the fit of the model by reconsidering the choice of factors, or determining the other source of error and holding it constant throughout all the designs. In the case of the installed power of the catamaran, the "Prob > F" combined with the R squared value of 1.00 indicates an excellent model. Similar results are found for the full load displacement response, where the R squared valued is 1.00 and the "Prob > F" is less than 0.0001 [11].

Table 4: Analysis of Variance Table

Source	DF	Sum of Squares	Mean Square	F Ratio
Model	9	1122424479	124713831	952.116616
Error	5	654929.39	130985.878	Prob > F
C. Total	14	1123079409	.	0.0001

Balancing a few additional point designs can further demonstrate the accuracy of the response surface equations. The responses from three additional point designs from different regions of the design space are compared to the predictions of the response

surface equations in Table 5. In all cases, the error is much less than 1%, verifying the accuracy of the curve fit.

Table 5: Comparison of Actual and Predicted Responses

	Variant A	Variant B	Variant C
Speed (kts)	35	49	47
Payload (lton)	150	110	185
Range (nm)	1000	1400	1900
Actual Installed Power (hp)	15316.3	20346.9	36555.6
Predicted Installed Power (hp)	15336.9	20319.2	36509.2
Installed Power % Difference	0.13 %	0.14 %	0.13 %
Actual Full Load Displacement (lton)	628.1	505.2	969.4
Predicted Full Load Displacement (lton)	627.8	504.1	967.9
Full Load Displacement % Difference	0.04 %	0.22 %	0.15 %

3.2.2 Design Space Visualization

The set of response surface equations allows the designer to predict the responses at any point in the design space. While this is an important benefit in itself, it also leads to the ability to visualize the entire design space, and determine what regions are feasible based on different sets of constraints. The contour plot in Figure 14 shows the contours of the installed power and full load displacement in the speed-range plane. In this figure, the payload is fixed at 150 ltons, and the full load displacement curve represents all the speed-range combinations that yield a full load displacement of 750 ltons. Similarly, the installed power curve represents all combinations leading to an installed power of 28,000 hp.

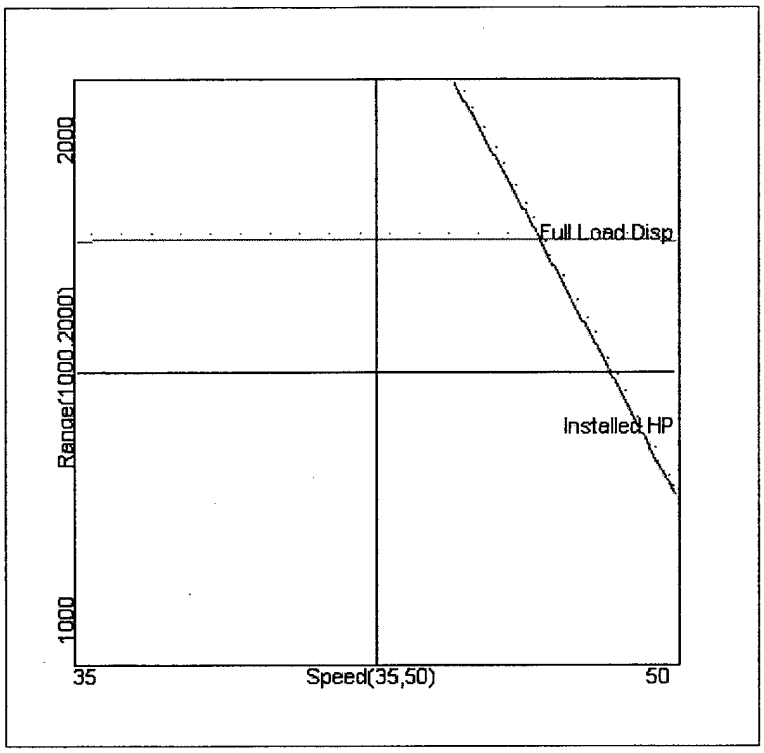

Figure 14: Catamaran Contour Plot (Payload = 150 lton, Full Load Displacement = 750 lton, Installed Power = 28,000 hp)

Figure 15 shows the same contour plot, but this time the designer has set some constraints on the design. In this case, the maximum acceptable installed power is 28,000 hp, and the maximum acceptable displacement is 750 ltons. Any points where the predicted responses exceed these limits are shaded, indicating that those points are no longer feasible. The feasible design space has been reduced to include only the white area of the plot.

Using a plot like this, it is easy to demonstrate the impacts of constraints and requirements on the design. For example, if the customer prescribes limits of 28,000 hp and 750 ltons, but wants the ship to carry 150 ltons of payload, go 50 kts and have a range of 1500 nm, the designer can easily show that this point is not in the feasible design space. It is easily seen that reducing the speed requirement to 48 kts or reducing the

range requirement to 1275 nm moves the design back into the feasible region. Similarly, the contour plot in the payload-range plane with speed fixed at 50 kts shows that reducing the payload requirement to 140 ltons also has the effect of moving the point back into the feasible design space, as illustrated in Figure 16.

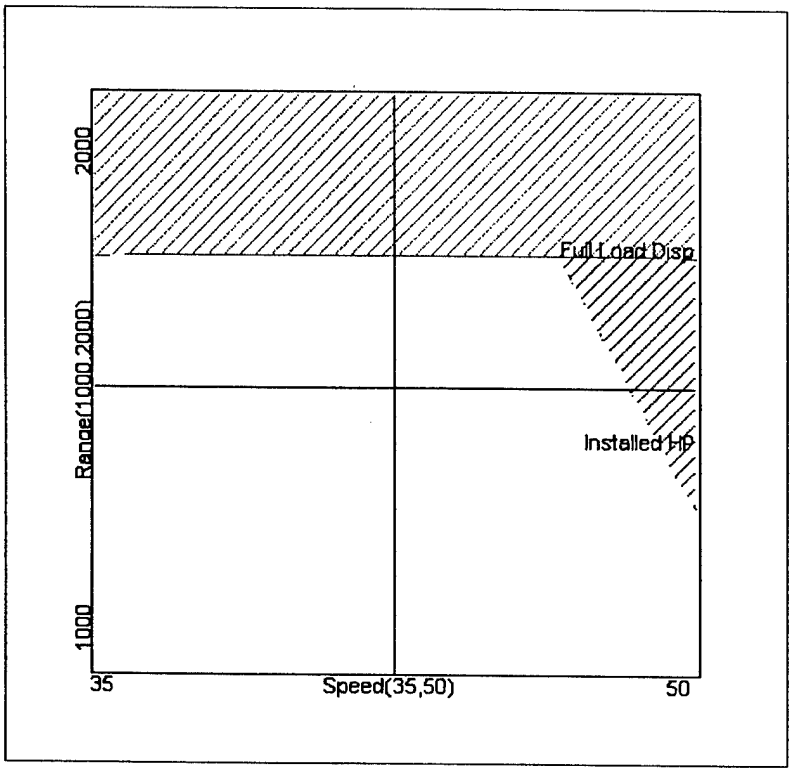

Figure 15: Catamaran Contour Plot (Payload = 150 lton, Full Load Displacement = 750 lton, Installed Power = 28,000 hp)

The effects of changing the constraints on the responses can also be investigated using the contour plot. Varying the upper limit for full load displacement and /or installed power changes the shape and size of the feasible design space.

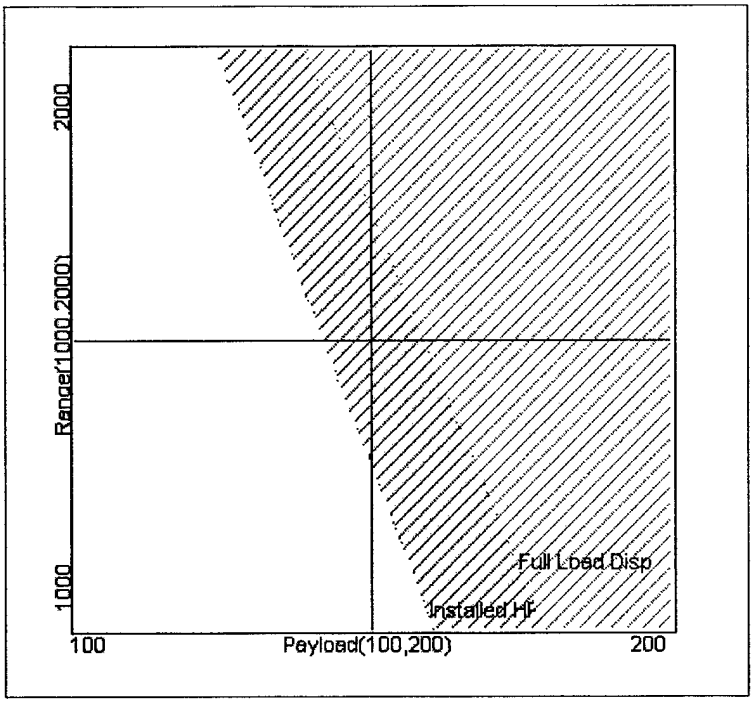

Figure 16: Catamaran Contour Plot (Speed = 50 kts, Full Load Displacement = 750 lton, Installed Power = 28,000 hp)

3.3 Benefits of RSM in Concept Exploration

The benefits of applying response surface methods to the concept exploration phase of the ship design process are numerous. Using the response surface equations, the responses for hundreds of designs can be easily estimated. This technique is very useful for determining the location of the Pareto boundary on the OMOE vs. Cost plot. Additionally, it is easy to estimate the effects of changing one or more factors in a point design. This allows the designer to answer a range of "what-if" questions without balancing another point design.

Finally, the contour plot provides an easily understandable display of the design space. The designer can not only pinpoint the factors that could be changed to meet the constraints, but also estimate how much each would have to be changed by. As in the

example in the previous section, instead of telling the customer that the constraints can be satisfied by reducing speed or range or payload, the designer can now predict that they will be satisfied by reducing speed by 2 kts or reducing range by 225 nm or reducing payload by 10 ltons. This provides a tremendous amount of additional information to the decision-maker, with little impact on the workload of the designer.

CHAPTER 4: INTEGRATING RSM AND UNCERTAINTY ANALYSIS

The previous two chapters have described the basics of RSM and uncertainty analysis. This chapter describes a process for integration into ship concept exploration. The process is best described through an example.

4.1 PROBLEM SET-UP

In this example, two different hull forms will be compared to determine which is more suitable for use as a littoral craft. To simplify the process, the requirements have already been translated into three attributes, which will be used as factors. Each attribute has a threshold value, which is the minimum requirement, and a goal value, which is the maximum that it could possibly need. In this case, Table 6 shows the goals and thresholds for the littoral craft.

Table 6: Goal and Threshold Values

Attribute	Threshold	Goal
Payload	100 lton	200 lton
Speed	35 kts	50 kts
Range	1000 nm	2000 nm

The factors are the attributes listed in the table, and in each case, the lower limit is the threshold value and the upper limit is the goal value. Since there is no continuous transition between a catamaran and a surface effect ship (SES), two separate design spaces must be examined. The factors listed in Table 6 define both design spaces. Table 7 shows the central composite variants that must be balanced for each hull form.

Table 7: DOE Variants

Variant	Pattern	Speed	Payload	Range
1	---	35	100	1000
2	--+	35	100	2000
3	a00	35	150	1500
4	-+-	35	200	1000
5	-++	35	200	2000
6	0a0	42.5	100	1500
7	00a	42.5	150	1000
8	0	42.5	150	1500
9	00A	42.5	150	2000
10	0A0	42.5	200	1500
11	+--	50	100	1000
12	+-+	50	100	2000
13	A00	50	150	1500
14	++-	50	200	1000
15	+++	50	200	2000

4.2 Determining Responses: Synthesis Model

The responses in this example are installed power, full load displacement, cost and OMOE. In order to show the uncertainty in the synthesis model, each response will be represented by a probability distribution instead of a single value. The synthesis model must be able to provide this information. Since the purpose of this study is to illustrate the method for integrating uncertainty analysis and RSM into concept exploration, a very simple Microsoft® Excel spreadsheet is used as the synthesis model. Crystal Ball® performs a Monte Carlo simulation, similar to the resistance model discussed in Chapter 2. The model uses deadweight fractions and speed-power data from existing ships to determine the full load displacement and installed power of each ship. Since there is a wide variation in the deadweight fractions among catamarans and SES, the deadweight fraction for each type of ship is assigned a uniform distribution. Additionally, speed-power curves were created based on existing ship data. The model

uses the values predicted by this curve as the most likely value and assigns a triangular distribution between +/- 20% of the most likely value to the shaft horsepower. The Monte Carlo simulation creates a probability distribution for each response, similar to the installed power distribution in Figure 17.

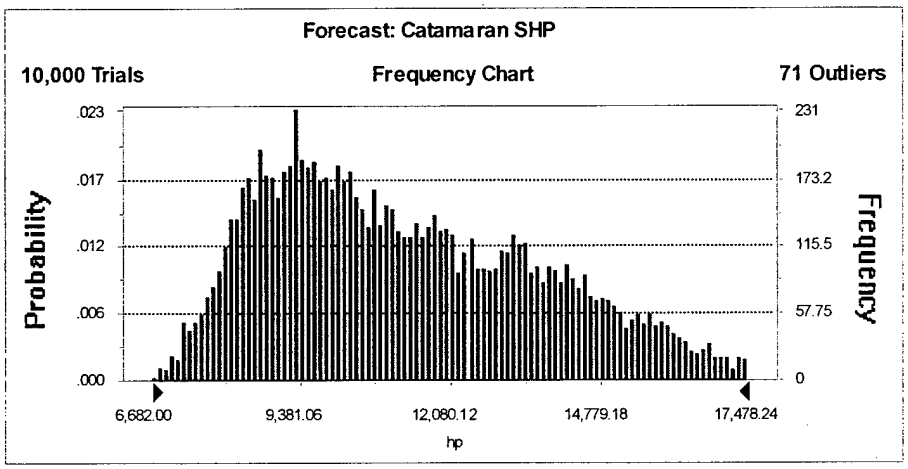

Figure 17: Catamaran Installed Power (Payload = 100 lton, Speed = 35 kts, Range = 1000 nm)

In order to create response surfaces using JMP®, the response must contain a discrete value. It is easy to see that in the 10,000 trials for this variant, there is an upper and lower limit for installed power. The upper and lower limits for the response provide two discrete points, but they do not define any probability for achieving the values in between. Instead of using the frequency chart, it is more useful to think about the responses in terms of a cumulative chart, illustrated in Figure 18. At any given power on the x-axis, the cumulative chart displays the probability of the power being less than or equal to that value. In this context, there is 0% chance of having an installed power less

than the lower limit and 100% chance of having an installed power of less than the upper limit.

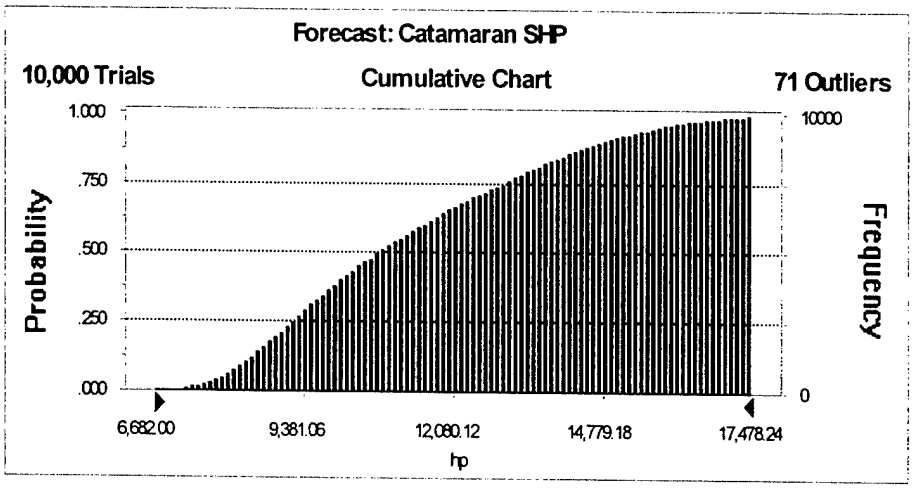

Figure 18: Installed Power Required Cumulative Distribution

Table 8 breaks the cumulative chart into 10% intervals and provides a series of values that describe the installed power cumulative distribution. (The differences between the lower limit of 6,682 hp on the cumulative chart and 6,574 hp in the percentile table can be attributed to the 71 outliers listed in the upper right corner of Figure 18. The same is true for the upper limit.) A table like this one is created to describe the installed power of each variant. Now, instead of representing installed power with a single surface, it can now be represented by a series of eleven separate surfaces that indicate different chances of installed power being less than or equal to a given value. Similar tables exist for the full load displacement and cost of the ship. In all three of these cases, it is desirable to minimize the installed power, full load displacement, and cost of the ship.

Table 8: Percentiles for Catamaran Installed Power (Payload = 100 lton, Speed = 35 kts, Range = 1000 nm)

Percentiles	Catamaran SHP
0%	6,574.11
10%	8,361.23
20%	8,988.91
30%	9,557.82
40%	10,168.27
50%	10,863.39
60%	11,675.14
70%	12,573.13
80%	13,590.33
90%	14,868.98
100%	19,022.92

The OMOE response must be handled a little differently, because it is more desirable to maximize OMOE. The OMOE is best understood in the context of a reverse cumulative chart, shown in Figure 19, which displays the probability of achieving an OMOE greater than or equal to any given value on the x-axis. The OMOE values for every 10% interval on the reverse cumulative chart can be put into a table similar to Table 8. Appendices A and B show the response data for each variant.

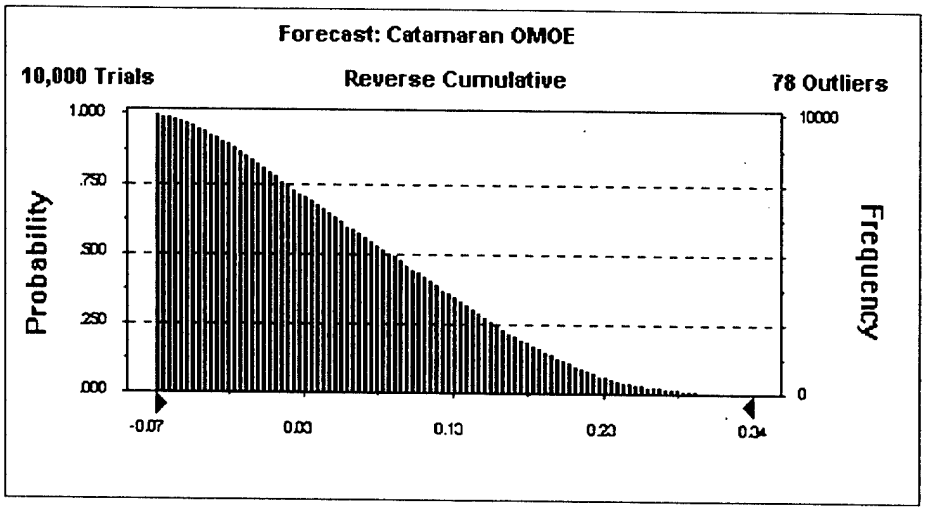

Figure 19: Catamaran OMOE Reverse Cummulative Chart (Payload = 100 lton, Speed = 35 kts, Range = 1000 nm)

4.3 APPLYING RSM

Representing each response by a series of numbers requires a significant increase in the data required. For this reason, organization of the data is very important. The four main responses, installed power, full load displacement, cost and OMOE are each divided into eleven sub-responses, one for each percentile listed in Table 8. The fit model in JMP® can determine the equation of a surface for each sub-response. It is important to check the R squared value and "Prob > F" discussed in Chapter 3 to ensure the surface fits the data. In this example, all the curve fits were excellent, with R-squared values of greater than 0.98 and "Prob > F" of less than 0.0001.

Displaying the results is a little more difficult, as well. In the contour plot created by JMP®, each sub-response has its own contour that moves independently of the others. In order to create a meaningful picture, each contour must be viewed in relation to the same installed power, meaning that each contour shows a different probability of

requiring an installed power of less than or equal to the same value. The only way to accomplish this in JMP® is to manually set this value for each contour. When this has been done, the contours create a band across the plot, as expected, but it is a very cumbersome process to change the installed power of interest. For this reason, the response surface equations from JMP® are re-created in a Microsoft® Excel spreadsheet, where the contours can be linked together. The resulting contour plot is shown in Figure 20. In this figure, it is easy to see that a catamaran with an installed power of 40,000 hp will almost certainly achieve a speed of 50 kts with a payload of 120 lton and a range of 1100 nm. Similarly, there is less than a 20% chance of a catamaran with 40,000 hp, a payload of 200 lton and a range of 2000 nm achieving a speed of 50 kts. Changing the maximum acceptable installed power causes all of the contour bands to shift, showing a different feasible design space.

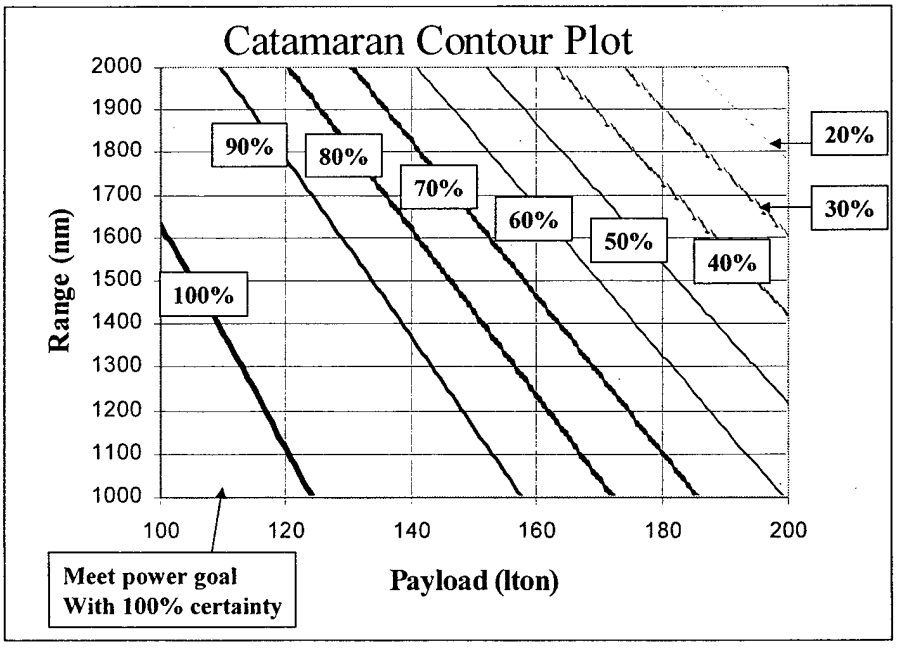

Figure 20: Catamaran Contour Plot (Speed = 50 kts, Max Acceptable Installed Power = 40,000 hp)

4.4 Interpreting Results

The method described above yields a great deal of information about the design space, but it does not help the decision maker if it cannot be interpreted and presented in a useful format. The following sections suggest some different formats for displaying the uncertainty and RSM data.

4.4.1 Contour Plot Comparison

The contour plot can provide a wealth of information about which designs are feasible. When the uncertainty bands are added, as in Figure 20, the decision maker can see how feasible each design is. This can be a great benefit when trying to trade-off two different hull types. Figure 21 shows the catamaran and SES contour plots side by side. Both are at a speed of 50 kts, and both have a maximum acceptable installed power of 40,000 hp. Obviously, the catamaran has a much larger feasible space than the SES. In fact, there is some probability of achieving a feasible design for a catamaran with a 50-kt speed and 40,000 hp installed for any payload-range combination in the design space. On the other hand, there is no chance of achieving a balanced SES design meeting the same speed and power criteria for all payload-range combinations above the 0% contour in the upper right corner of the SES plot. Note that the 50% contour is approximately the same as the most likely value band, or the band that would be displayed if uncertainty were not included in the synthesis model.

In the event that achieving a 50-kt speed with the minimum installed power is the only criteria for choosing a hull type, the catamaran is the obvious winner. If, however, speed and installed power are secondary in importance to other criteria, the SES may remain competitive. Figure 21 shows that there is a chance of achieving balanced

designs over most of the design space, but they are much less probable than those of the catamaran. When speed and power are not the primary concern, but could be a secondary benefit, the SES could be a valid choice. The contour plot allows the decision maker to see exactly what the chances are of creating a balanced design for any speed-payload-range combination.

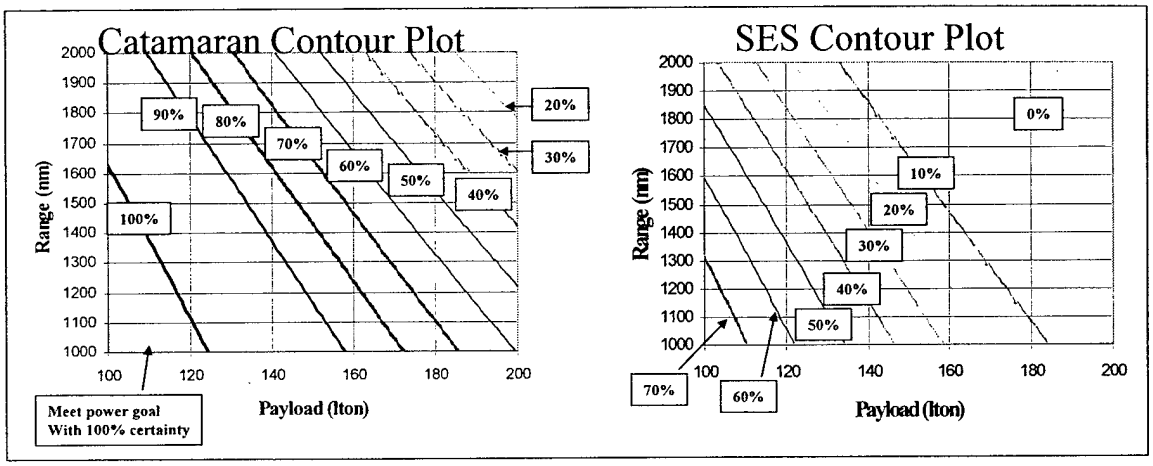

Figure 21: Comparison of Catamaran and SES Contour Plots (Speed = 50 kts, Max Acceptable Installed Power = 40,000 hp)

One of the biggest difficulties in comparing designs created using different synthesis models is the lack of information concerning the assumptions involved. Some models may predict extremely optimistic designs, while others take a much more conservative approach. It is nearly impossible to compare designs from such different models without analyzing the uncertainty involved in each. The plots in Figure 21 are also useful in determining the feasibility of designs synthesized using other models. When the decision maker has contour plots like these that he has great confidence in, it is easy to evaluate other designs. For example, if a designer claims that a catamaran with a

speed of 50 kts, payload of 200 lton, range of 2000 nm and installed power of 40,000 hp can be realized, the decision-maker can easily see that while this design is possible, according to Figure 21, it is not very probable. This could indicate that the designer has made some very optimistic assumptions that may not hold up throughout the design process.

4.4.2 OMOE vs. Cost Plot

Incorporating the uncertainty bands in the contour plot into the OMOE vs. cost plot can provide another useful comparison technique. In the plot in Figure 22, the cost and OMOE of three different catamaran point designs are plotted. The factors (speed, payload, and range) for each variant are as follows:

Variant A: 50 kts, 100 lton, 2000 nm

Variant B: 50 kts, 150 lton, 1500 nm

Variant C: 35 kts, 200 lton, 1000 nm

The "x" in each case, represents the solution that will occur with 100% certainty. This represents the lowest OMOE and highest cost, or worst possible case for the design. Moving out from this point, each band represents a decreasing level of certainty of achieving that point. Notice that in all cases, these bands move the design closer to the ideal point. Even though there is some overlap between variant C and the other two variants, it is so small that variants A and B will almost certainly dominate variant C, so variant C can be ruled out. The decision between variants A and B is not as clear cut, however, due to the large amount of overlap between the designs. This could indicate that cost and OMOE alone are not good discriminators between the two designs, and the decision should be based on other criteria.

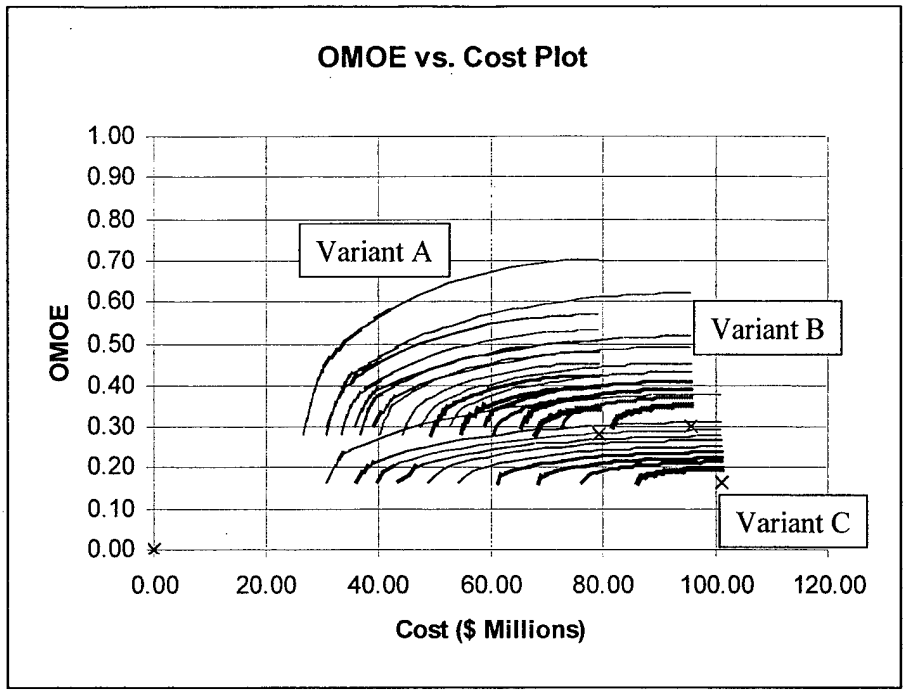

Figure 22: OMOE vs. Cost Plot with Uncertainty Bands

Chapter 2 pointed out the fact that the response surface equations could be used to estimate the cost and OMOE of hundreds of different variants. With such a large number of points that are spanning the entire design space, the Pareto boundary on the OMOE vs. Cost plot should become very clear. Figure 23 shows the Pareto boundaries at a 100% and 0% certainty level for the catamaran and SES. At the 100% certainty level, the catamaran Pareto boundary clearly dominates the SES boundary, but at the 0% certainty level they are almost indistinguishable. This indicates that there will be considerable overlap in the point designs, again indicating that cost and OMOE alone may not lead to clear-cut decision.

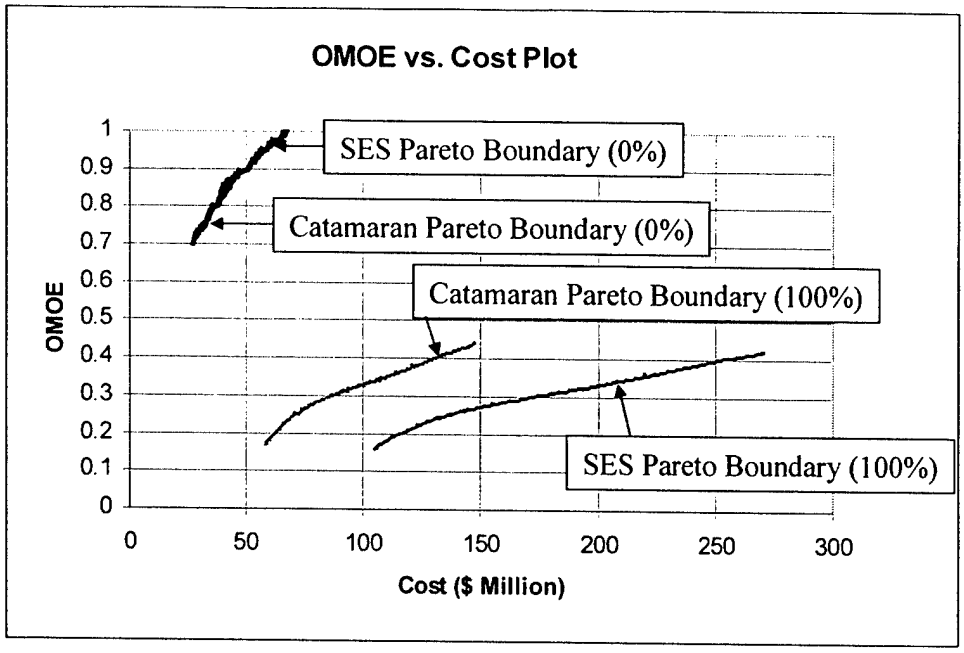

Figure 23: OMOE vs. Cost Plot showing Pareto Boundaries

CHAPTER 5: CONCLUSIONS AND RECOMMENDATIONS

The integration of response surface methods and uncertainty analysis into ship concept exploration can improve the early stage ship design process tremendously, by aiding the decision-maker in navigating the complex design space and arriving at a baseline design that will lead to a cost-effective ship.

5.1 CONCLUSIONS

The combination of uncertainty analysis with RSM and DOE, as well as the OMOE vs. Cost plot can provide the decision-maker with a great deal of information during ship concept exploration. Adopting the uncertainty analysis using a Monte Carlo simulation allows the designer to better understand the uncertainty involved in the synthesis model. This can lead to the elimination or adjustment of certain margins based on the distribution of the data. Also, the decision-maker can benefit from understanding the probability of achieving different design points.

Design of Experiments provides a systematic method of choosing point designs that span the entire design space, ensuring that all possibilities are considered. Response Surface Methods allow the designer to make predictions about any ship in the design space using the combination of factors. Rapid generation of predicted responses can help define the Pareto boundary on the OMOE vs. Cost plot, as well as answer a multitude of "what-if" questions about the designs.

Perhaps the greatest benefit of integrating RSM and uncertainty analysis into ship concept exploration is the ability to determine whether or not certain metrics can discriminate between two designs. While it seems that this discovery is contrary to

making a decision, it could actually be very useful. If the decision-maker knows that the OMOE vs. cost plot cannot really discriminate between a catamaran and SES, he is free to make a decision based on other criteria.

5.2 Recommendations for Future Study

This study highlighted several areas that require further study to make the concept exploration phase more effective. As mentioned in Chapter 2, it would be interesting to investigate the uncertainty involved in the OMOE model itself. This would require looking at the world's changing geopolitical environment, as well as dealing with the lack of agreement on the part of the customer. The lack of agreement manifests itself due to Arrow's Impossibility Theorem that states there is no utility function that can successfully model the preferences of a group of decision makers [12]. Modeling the uncertainty in individual decision maker preferences could lead to models that can allow interactive decision maker negotiation, since the negotiation requires rapidly changing the form of the ship design solution in a group negotiation environment. The uncertainty-RSM metamodels can rapidly produce ship solutions as the decision makers negotiate to a solution.

Additionally, this study did not address the translation of requirements into a set of factors and responses. This is a crucial step in the process, and can be extremely challenging. Currently, no process or guidelines exist to aid in this task.

In order to effectively use the method described in this paper, a great deal of effort needs to go into developing advanced hull form models that provide uncertainty data. There is currently a shortage of synthesis models for ships with advanced hull forms, and there is a great deal of uncertainty associated with them. Quantifying the uncertainty in

the synthesis models, for both monohulls and advanced hull forms, is an important part of making this method useful.

Finally, displaying the results of this method is not a trivial task. This paper suggests several ways of plotting data that may be useful to the decision-maker, but there are countless others. It can be difficult to predict what information is most valuable to the decision-maker, because it may be different for each individual, and also for each project. Feedback from decision-makers would be extremely helpful in developing easily understandable and useful plots.

REFERENCES

[1] Brown, David K. 1993. Naval Architecture. *Naval Engineers Journal* (Jan): 42-50.

[2] Bebar, M. and R. Finney. 1999. Reinventing Naval Ship Design: Partnerships, Innovation, and Systems Engineering. *Naval Engineers Journal* (May): 325-334.

[3] Brown, Alan and Mark Thomas. 1998. Reengineering the Naval Ship Concept Design Process. In *From Research to Reality in Ship Systems Engineering, September 18-19, 1998,* by American Society of Naval Engineers.

[4] Evans, J. Harvey. 1959. Basic Design Concepts. *ASNE Journal* (November): 671-675.

[5] Whitcomb, C.A. 1998. Naval Ship Design Philosophy Implementation. *Naval Engineers Journal* (January): 49-63.

[6] Gertler, Morton. 1954. *A Reanalysis of the Original Test Data for the Taylor Standard Series.* David Taylor Model Basin Report 806.

[7] Schmidt, Stephen and Robert Launsby. 1998. *Understanding Industrial Designed Experiments,* 4th ed. Colorado Springs: Air Academy Press.

[8] Box, G., W. Hunter and J. Hunter. 1978. *Statistics for Experimenters: An Introduction to Design, Data Analysis, and Model Building.* John Wiley and Sons.

[9] Goggins, David. 2001. Response Surface Methods Applied to Submarine Concept Exploration. Master of Science thesis, Massachusetts Institute of Technology.

[10] SAS Institute. 2000. *JMP® Design of Experiments, Version 4.* Cary, NC: SAS Institute.

[11] SAS Institute. 2000. *JMP® Statistics and Graphics Guide, Version 4.* Cary, NC: SAS Institute.

[12] Whitcomb, C.A. 1998. A Prescriptive Production-Distribution Approach to Decision Making in New Product Design. Ph.D. Dissertation, University of Maryland.

APPENDIX A: CATAMARAN POINT DESIGN DATA

SHP: Probability that result is less than given value

Variant	Pattern	Payload	Speed	Range	SHP 0	SHP 10	SHP 20	SHP 30
1	---	100	35	1000	6574	8361	8989	9558
2	--+	100	35	2000	9355	11899	12792	13602
3	a00	100	42.5	1500	10213	12989	13965	14848
4	-+-	100	50	1000	11214	14262	15333	16303
5	-++	100	50	2000	15958	20296	21820	23200
6	0a0	150	35	1500	11581	14729	15834	16836
7	00a	150	42.5	1000	13059	16609	17856	18986
8	000	150	42.5	1500	15336	19505	20970	22297
9	00A	150	42.5	2000	18584	23637	25411	27019
10	0A0	150	50	1500	19753	25123	27009	28718
11	+--	200	35	1000	13148	16722	17978	19116
12	+-+	200	35	2000	18711	23797	25584	27203
13	A00	200	42.5	1500	20426	25979	27929	29697
14	++-	200	50	1000	22427	28524	30665	32606
15	+++	200	50	2000	31916	40592	43639	46401

Variant	SHP 40	SHP 50	SHP 60	SHP 70	SHP 80	SHP 90	SHP 100
1	10168	10863	11675	12573	13590	14869	19023
2	14470	15459	16615	17893	19340	21160	27071
3	15797	16877	18138	19533	21113	23099	29553
4	17344	18530	19915	21446	23181	25362	32448
5	24682	26370	28340	30520	32989	36093	46176
6	17912	19136	20566	22148	23940	26192	33510
7	20199	21580	23192	24976	26997	29537	37789
8	23721	25343	27236	29331	31704	34687	44377
9	28745	30710	33005	35543	38419	42033	53776
10	30553	32641	35080	37779	40835	44677	57158
11	20337	21727	23350	25146	27181	29738	38046
12	28940	30919	33229	35785	38680	42319	54142
13	31593	33753	36275	39065	42226	46199	59105
14	34689	37060	39829	42893	46363	50725	64896
15	49365	52739	56680	61040	65978	72185	92352

Full Load Displacement: Probability that result is less than given value

Variant	Pattern	Payload	Speed	Range	FL 0	FL 10	FL 20	FL 30
1	---	100	35	1000	327.3	349.8	370.0	392.2
2	--+	100	35	2000	465.8	497.7	526.5	558.2
3	a00	100	42.5	1500	384.0	410.3	434.0	460.1
4	-+-	100	50	1000	327.3	349.8	370.0	392.2
5	-++	100	50	2000	465.8	497.7	526.5	558.2
6	0a0	150	35	1500	576.6	616.1	651.8	690.9
7	00a	150	42.5	1000	491.0	524.6	555.0	588.4
8	000	150	42.5	1500	576.6	616.1	651.8	690.9
9	00A	150	42.5	2000	698.7	746.6	789.8	837.3
10	0A0	150	50	1500	576.6	616.1	651.8	690.9
11	+--	200	35	1000	654.7	699.5	740.0	784.5
12	+-+	200	35	2000	931.6	995.4	1053.1	1116.4
13	A00	200	42.5	1500	768.0	820.6	868.1	920.2
14	++-	200	50	1000	654.7	699.5	740.0	784.5
15	+++	200	50	2000	931.6	995.4	1053.1	1116.4

Variant	FL 40	FL 50	FL 60	FL 70	FL 80	FL 90	FL 100
1	416.7	444.5	478.2	515.5	556.3	605.5	675.1
2	593.0	632.5	680.6	733.5	791.6	861.6	960.7
3	488.8	521.4	561.0	604.7	652.6	710.3	791.9
4	416.7	444.5	478.2	515.5	556.3	605.5	675.1
5	593.0	632.5	680.6	733.5	791.6	861.6	960.7
6	734.0	782.9	842.4	908.0	979.9	1066.6	1189.2
7	625.0	666.7	717.3	773.2	834.4	908.2	1012.7
8	734.0	782.9	842.4	908.0	979.9	1066.6	1189.2
9	889.5	948.7	1020.8	1100.3	1187.4	1292.4	1441.1
10	734.0	782.9	842.4	908.0	979.9	1066.6	1189.2
11	833.4	888.9	956.5	1030.9	1112.6	1210.9	1350.2
12	1186.0	1265.0	1361.1	1467.1	1583.2	1723.3	1921.5
13	977.6	1042.8	1122.0	1209.3	1305.1	1420.5	1583.9
14	833.4	888.9	956.5	1030.9	1112.6	1210.9	1350.2
15	1186.0	1265.0	1361.1	1467.1	1583.2	1723.3	1921.5

Cost: Probability that result is less than given value

Variant	Pattern	Payload	Speed	Range	Cost 0	Cost 10	Cost 20	Cost 30
1	---	100	35	1000	19.35	22.01	24.03	26.13
2	--+	100	35	2000	24.21	27.98	30.83	33.80
3	a00	100	42.5	1500	22.22	25.43	27.84	30.34
4	-+-	100	50	1000	20.93	23.81	25.91	28.11
5	-++	100	50	2000	26.35	30.38	33.33	36.44
6	0a0	150	35	1500	28.05	32.69	36.21	39.87
7	00a	150	42.5	1000	26.16	30.23	33.30	36.46
8	000	150	42.5	1500	29.26	34.04	37.64	41.32
9	00A	150	42.5	2000	33.65	39.41	43.75	48.23
10	0A0	150	50	1500	30.62	35.54	39.19	42.98
11	+--	200	35	1000	30.73	35.98	39.97	44.12
12	+-+	200	35	2000	40.12	47.55	53.18	59.09
13	A00	200	42.5	1500	36.12	42.44	47.19	52.11
14	++-	200	50	1000	33.58	39.14	43.28	47.57
15	+++	200	50	2000	43.91	51.74	57.60	63.63

Variant	Cost 40	Cost 50	Cost 60	Cost 70	Cost 80	Cost 90	Cost 100
1	28.71	31.45	34.78	38.48	42.52	47.45	55.05
2	37.45	41.33	46.04	51.25	56.99	63.95	74.69
3	33.41	36.69	40.68	45.05	49.87	55.76	64.84
4	30.78	33.66	37.15	40.90	45.14	50.30	58.27
5	40.22	44.26	49.16	54.50	60.46	67.73	78.98
6	44.36	49.15	54.95	61.39	68.47	77.05	90.31
7	40.38	44.55	49.63	55.20	61.33	68.82	80.36
8	45.92	50.78	56.73	63.25	70.44	79.21	92.71
9	53.75	59.64	66.80	74.69	83.37	93.92	110.25
10	47.66	52.64	58.68	65.26	72.64	81.55	95.40
11	49.21	54.63	61.21	68.51	76.53	86.24	101.27
12	66.28	73.95	83.23	93.58	104.95	118.65	139.94
13	58.17	64.62	72.48	81.14	90.66	102.24	120.16
14	52.87	58.50	65.32	72.81	81.15	91.25	106.91
15	71.13	79.09	88.69	99.34	111.05	125.34	147.45

Normalized OMOE: Probability that result is greater than given value

Variant	Pattern	Payload	Speed	Range	OMOE 0	OMOE 10	OMOE 20	OMOE 30
1	---	100	35	1000	0.223	0.152	0.133	0.119
2	--+	100	35	2000	0.547	0.414	0.376	0.347
3	a00	100	42.5	1500	0.461	0.361	0.333	0.314
4	-+-	100	50	1000	0.380	0.314	0.295	0.280
5	-++	100	50	2000	0.704	0.571	0.533	0.504
6	0a0	150	35	1500	0.466	0.361	0.333	0.314
7	00a	150	42.5	1000	0.380	0.314	0.295	0.280
8	000	150	42.5	1500	0.542	0.442	0.414	0.390
9	00A	150	42.5	2000	0.704	0.571	0.533	0.504
10	0A0	150	50	1500	0.623	0.518	0.495	0.471
11	+--	200	35	1000	0.380	0.314	0.295	0.280
12	+-+	200	35	2000	0.704	0.571	0.533	0.504
13	A00	200	42.5	1500	0.623	0.518	0.490	0.471
14	++-	200	50	1000	0.538	0.471	0.452	0.438
15	+++	200	50	2000	0.866	0.728	0.690	0.666

Variant	OMOE 40	OMOE 50	OMOE 60	OMOE 70	OMOE 80	OMOE 90	OMOE 100
1	0.109	0.095	0.081	0.066	0.052	0.038	0.009
2	0.319	0.295	0.266	0.238	0.214	0.185	0.123
3	0.290	0.271	0.252	0.233	0.209	0.190	0.142
4	0.266	0.252	0.238	0.223	0.214	0.200	0.166
5	0.480	0.452	0.423	0.395	0.371	0.342	0.280
6	0.295	0.271	0.252	0.233	0.214	0.190	0.142
7	0.266	0.252	0.238	0.223	0.214	0.200	0.166
8	0.371	0.352	0.333	0.309	0.290	0.271	0.223
9	0.480	0.452	0.423	0.395	0.371	0.342	0.280
10	0.452	0.433	0.409	0.390	0.371	0.352	0.304
11	0.266	0.252	0.238	0.223	0.214	0.200	0.166
12	0.480	0.452	0.423	0.395	0.371	0.342	0.280
13	0.452	0.428	0.409	0.390	0.371	0.347	0.304
14	0.423	0.409	0.395	0.385	0.371	0.357	0.323
15	0.637	0.609	0.580	0.557	0.528	0.504	0.438

Page intentionally left blank

APPENDIX B: SES POINT DESIGN DATA

SHP: Probability that result is less than given value

Variant	Pattern	Payload	Speed	Range	SHP 0	SHP 10	SHP 20	SHP 30
1	---	100	35	1000	8212	10604	11511	12407
2	--+	100	35	2000	11419	14746	16007	17254
3	a00	100	42.5	1500	14085	18189	19744	21282
4	-+-	100	50	1000	16740	21617	23466	25293
5	-++	100	50	2000	23279	30061	32632	35173
6	0a0	150	35	1500	14306	18474	20054	21615
7	00a	150	42.5	1000	18150	23438	25442	27423
8	000	150	42.5	1500	21081	27222	29550	31851
9	00A	150	42.5	2000	25240	32593	35381	38136
10	0A0	150	50	1500	29164	37661	40881	44065
11	+--	200	35	1000	16423	21208	23021	24814
12	+-+	200	35	2000	22838	29492	32014	34507
13	A00	200	42.5	1500	28170	36377	39488	42563
14	++-	200	50	1000	33480	43234	46931	50586
15	+++	200	50	2000	46558	60122	65263	70346

Variant	SHP 40	SHP 50	SHP 60	SHP 70	SHP 80	SHP 90	SHP 100
1	13461	14712	16265	18085	20237	23039	31133
2	18719	20458	22618	25150	28142	32039	43295
3	23090	25235	27899	31021	34712	39519	53402
4	27441	29991	33157	36868	41255	46968	63468
5	38161	41706	46109	51270	57370	65314	88260
6	23452	25630	28336	31508	35257	40139	54240
7	29753	32517	35950	39974	44730	50924	68814
8	34557	37767	41755	46428	51952	59146	79925
9	41375	45219	49994	55589	62203	70816	95694
10	47808	52249	57766	64231	71874	81826	110572
11	26922	29423	32530	36170	40474	46079	62266
12	37439	40916	45237	50299	56284	64078	86589
13	46179	50469	55798	62043	69425	79038	106805
14	54883	59981	66315	73736	82510	93935	126935
15	76322	83412	92219	102539	114740	130628	176519

Full Load Displacement: Probability that result is less than given value

Variant	Pattern	Payload	Speed	Range	FL 0	FL 10	FL 20	FL 30
1	---	100	35	1000	403.0	436.2	468.6	505.1
2	--+	100	35	2000	560.4	606.6	651.6	702.5
3	a00	100	42.5	1500	469.1	507.7	545.5	588.0
4	-+-	100	50	1000	403.0	436.2	468.6	505.1
5	-++	100	50	2000	560.4	606.6	651.6	702.5
6	0a0	150	35	1500	702.1	759.9	816.4	880.1
7	00a	150	42.5	1000	604.5	654.3	702.9	757.7
8	000	150	42.5	1500	702.1	759.9	816.4	880.1
9	00A	150	42.5	2000	840.7	909.8	977.4	1053.7
10	0A0	150	50	1500	702.1	759.9	816.4	880.1
11	+--	200	35	1000	806.0	872.3	937.2	1010.3
12	+-+	200	35	2000	1120.9	1213.1	1303.2	1404.9
13	A00	200	42.5	1500	938.3	1015.5	1090.9	1176.0
14	++-	200	50	1000	806.0	872.3	937.2	1010.3
15	+++	200	50	2000	1120.9	1213.1	1303.2	1404.9

Variant	FL 40	FL 50	FL 60	FL 70	FL 80	FL 90	FL 100
1	547.2	596.9	661.3	735.2	823.3	937.3	1107.8
2	761.0	830.1	919.7	1022.4	1144.9	1303.4	1540.5
3	637.0	694.8	769.8	855.8	958.4	1091.1	1289.5
4	547.2	596.9	661.3	735.2	823.3	937.3	1107.8
5	761.0	830.1	919.7	1022.4	1144.9	1303.4	1540.5
6	953.4	1039.9	1152.2	1280.8	1434.3	1632.9	1930.0
7	820.8	895.3	992.0	1102.8	1235.0	1405.9	1661.7
8	953.4	1039.9	1152.2	1280.8	1434.3	1632.9	1930.0
9	1141.5	1245.1	1379.5	1533.5	1717.4	1955.1	2310.8
10	953.4	1039.9	1152.2	1280.8	1434.3	1632.9	1930.0
11	1094.5	1193.8	1322.7	1470.3	1646.6	1874.6	2215.6
12	1522.0	1660.1	1839.3	2044.7	2289.8	2606.8	3081.0
13	1274.0	1389.7	1539.6	1711.6	1916.7	2182.1	2579.1
14	1094.5	1193.8	1322.7	1470.3	1646.6	1874.6	2215.6
15	1522.0	1660.1	1839.3	2044.7	2289.8	2606.8	3081.0

Cost: Probability that result is less than given value

Variant	Pattern	Payload	Speed	Range	Cost 0	Cost 10	Cost 20	Cost 30
1	---	100	35	1000	27.28	31.03	34.23	37.75
2	--+	100	35	2000	34.79	39.97	44.42	49.29
3	a00	100	42.5	1500	31.91	36.49	40.32	44.47
4	-+-	100	50	1000	29.90	34.16	37.57	41.26
5	-++	100	50	2000	38.27	44.06	48.77	53.86
6	0a0	150	35	1500	41.48	47.95	53.51	59.59
7	00a	150	42.5	1000	38.71	44.55	49.43	54.78
8	000	150	42.5	1500	43.57	50.30	55.95	62.14
9	00A	150	42.5	2000	50.42	58.43	65.18	72.57
10	0A0	150	50	1500	45.70	52.88	58.74	65.06
11	+--	200	35	1000	46.35	53.78	60.15	67.12
12	+-+	200	35	2000	60.97	71.30	80.08	89.76
13	A00	200	42.5	1500	55.21	64.12	71.64	79.88
14	++-	200	50	1000	51.10	59.29	65.99	73.20
15	+++	200	50	2000	67.30	78.50	87.72	97.68

Variant	Cost 40	Cost 50	Cost 60	Cost 70	Cost 80	Cost 90	Cost 100
1	42.11	47.04	53.35	60.69	69.27	80.60	97.87
2	55.30	62.14	70.80	81.00	92.82	108.50	132.48
3	49.67	55.56	62.96	71.80	82.03	95.52	116.14
4	45.87	51.08	57.67	65.45	74.52	86.48	104.92
5	60.20	67.40	76.49	87.25	99.69	116.20	141.60
6	67.11	75.61	86.44	99.17	113.92	133.54	163.47
7	61.44	68.99	78.49	89.81	102.91	120.19	146.62
8	69.86	78.62	89.65	102.72	117.88	137.88	168.50
9	81.76	92.20	105.35	120.94	139.08	162.93	199.42
10	72.97	81.92	93.22	106.67	122.16	142.68	174.35
11	75.72	85.44	97.87	112.43	129.33	151.83	186.14
12	101.63	115.05	132.31	152.46	175.84	206.97	254.54
13	90.11	101.73	116.41	133.74	153.93	180.52	221.14
14	82.26	92.50	105.45	120.84	138.58	162.04	198.24
15	110.22	124.31	142.14	163.43	187.88	220.23	270.19

Normalized OMOE: Probability that result is greater than given value

Variant	Pattern	Payload	Speed	Range	OMOE 0	OMOE 10	OMOE 20	OMOE 30
1	---	100	35	1000	0.285	0.200	0.176	0.157
2	--+	100	35	2000	0.685	0.504	0.457	0.419
3	a00	100	42.5	1500	0.566	0.433	0.395	0.366
4	-+-	100	50	1000	0.447	0.357	0.333	0.314
5	-++	100	50	2000	0.842	0.666	0.614	0.576
6	0a0	150	35	1500	0.561	0.428	0.395	0.361
7	00a	150	42.5	1000	0.447	0.357	0.333	0.314
8	000	150	42.5	1500	0.642	0.509	0.476	0.442
9	00A	150	42.5	2000	0.842	0.666	0.614	0.576
10	0A0	150	50	1500	0.723	0.590	0.552	0.523
11	+--	200	35	1000	0.447	0.357	0.333	0.314
12	+-+	200	35	2000	0.842	0.666	0.614	0.576
13	A00	200	42.5	1500	0.723	0.590	0.557	0.523
14	++-	200	50	1000	0.604	0.518	0.490	0.471
15	+++	200	50	2000	0.999	0.823	0.776	0.733

Variant	OMOE 40	OMOE 50	OMOE 60	OMOE 70	OMOE 80	OMOE 90	OMOE 100
1	0.133	0.114	0.095	0.071	0.052	0.033	0.000
2	0.376	0.333	0.295	0.252	0.214	0.176	0.100
3	0.333	0.304	0.271	0.242	0.214	0.185	0.128
4	0.295	0.271	0.252	0.233	0.214	0.195	0.157
5	0.533	0.495	0.452	0.409	0.371	0.333	0.261
6	0.333	0.304	0.271	0.242	0.214	0.185	0.128
7	0.295	0.271	0.252	0.233	0.214	0.195	0.157
8	0.414	0.380	0.352	0.319	0.290	0.261	0.209
9	0.533	0.495	0.452	0.409	0.371	0.333	0.261
10	0.490	0.461	0.428	0.399	0.371	0.342	0.285
11	0.295	0.271	0.252	0.233	0.214	0.195	0.157
12	0.533	0.495	0.452	0.409	0.371	0.333	0.261
13	0.495	0.461	0.433	0.399	0.371	0.342	0.290
14	0.452	0.433	0.409	0.390	0.371	0.352	0.314
15	0.695	0.652	0.609	0.571	0.533	0.495	0.419